1953

The crystal structure of two iodine-containing compounds

William Joseph James
Iowa State College

NOTE TO USERS

This reproduction is the best copy available.

UMI®

THE CRYSTAL STRUCTURE OF TWO IODINE-CONTAINING COMPOUNDS

by

William J. James

A Dissertation Submitted to the
Graduate Faculty in Partial Fulfillment of
The Requirements for the Degree of
DOCTOR OF PHILOSOPHY

Major Subject: Physical Chemistry

Approved:

Signature was redacted for privacy.

Signature was redacted for privacy.
In Charge of Major Work

Signature was redacted for privacy.
Head of Major Department

Signature was redacted for privacy.
Dean of Graduate College

Iowa State College

1953

TABLE OF CONTENTS

PART I.

STRUCTURE OF THE

CYCLOHEXAAMYLOSE–IODINE COMPLEX

INTRODUCTION

The iodine addition products of the Schardinger cyclic dextrins, because of their close analogy to the amylose-iodine complex, are of considerable importance as an aid to a more complete understanding of the physical and chemical properties of amylose and starch.

The concept of a helical configuration for starch has been useful in explaining several properties of the high polymer. A complete knowledge of the structure of a cycloamylose such as cyclohexaamylose (Schardinger's α-dextrin) would be of considerable value in the verification of the helical theory (1).

The location of the iodine atoms and the nature of the carbohydrate molecule in the cyclohexaamylose-iodine complex (Schardinger's α-dextrin-iodine complex) were reported by the author in a thesis submitted to the graduate faculty at Iowa State College (2). A brief account of this work is also found in the literature (3). On the basis of optical and X-ray studies, the structure was described as a torus-like arrangement of six cyclic glucoses, coaxial with and surrounding each iodine molecule. From a measurement of scale models and consideration of the possible packing arrangements, the approximate dimensions of the tori were determined.

Further studies here reported have been carried out to locate more exactly the positions of carbon and oxygen atoms. Although no progress can be reported in this respect, additional and more striking evidence for the cylindrical or torus-like nature of the carbohydrate molecule has been found.

The results of this study thus give additional support to the existence of the helical configuration of the amylose-iodine complex (1).

EXPERIMENTAL

Preparation of Isomorphous Complexes

An attempt was made to prepare crystals of cyclohexaamylose isomorphous with the iodine complex. The solvents used were 50 per cent solutions of aqueous n-propanol, ethanol, methanol, and water. Crystals prepared from the last two solvents tend to crack and become opaque when removed from the mother liquor. These crystals were coated with Canada balsam diluted with xylene in order to prevent the loss of hydrated solvent.

Diffraction Data

Crystals from the above mentioned solvents were mounted with the z axis normal to the X-ray beam. Ten-degree oscillation patterns were taken for alignment using Ni filtered CuKα radiation and a cylindrical camera of 57.3 mm. diameter. A complete rotation pattern together with a zero-layer Weissenberg pattern were used to obtain the lattice constants. The crystals obtained from n-propanol, ethanol, and methanol were most nearly isomorphous with the iodine complex. In the case of the latter two, the rate of loss of solvent appeared to vary with the crystals studied, so that the cell dimensions may be somewhat variable. The values obtained are compared with those of the iodine complex.

Iodine complex	n-propanol	ethanol	methanol
$a_o = 14.38 \pm 0.05$Å	$a_o = 14.24 \pm 0.05$Å	$a_o = 14.31$Å	$a_o = 13.94$Å
$b_o = 36.07 \pm 0.05$	$b_o = 37.30 \pm 0.05$	$b_o = 37.46$	$b_o = 36.83$
$c_o = 9.43 \pm 0.05$	$c_o = 9.43 \pm 0.05$	$c_o = 9.43$	$c_o = 9.47$

The crystals possess orthorhombic symmetry; Weissenberg and precession patterns revealed all odd orders of the (h00), (0k0), and (00ℓ) reflections missing. The space group is D_2^4 -- $P2_12_12_1$, requiring four molecules per unit cell. Space group data are shown in Fig. 1.

Intensity Data

Weissenberg films of (hk0) data timed to give a film factor of two were prepared from the methanol complex using Ni filtered CuKα radiation. Precession films of (0kℓ) data were obtained similarly using Zr filtered MoKα radiation. The films were developed simultaneously and the intensities estimated by visual comparison methods. Corrections for Lorentz and polarization factors resulted in relative values of F^2. No correction was necessary for absorption. The F^2 values of both the iodine and methanol complexes were then placed on an absolute scale using the method of A. J. C. Wilson (4). A brief discussion of the method follows.

The expression for intensity is given by

$$I(hk\ell) = \sum_\alpha \sum_\beta f_\alpha f_\beta \exp 2\pi i \left[h(x_\alpha - x_\beta) + k(y_\alpha - y_\beta) + \ell(z_\alpha - z_\beta)\right]$$

$$= \sum_\alpha f_\alpha^2 + \sum_{\alpha \neq \beta} \sum f_\alpha f_\beta \exp 2\pi i \left[h(x_\alpha - x_\beta) + k(y_\alpha - y_\beta) + \ell(z_\alpha - z_\beta)\right]$$

By arranging the $I(hk\ell)$ for all reflections in a given range of $\sin^2\theta/\lambda^2$ and provided that $\lambda/\sin\theta$ is small compared with interatomic distances, the exponential term in the above equation averages to a value of zero. To a first approximation, $\overline{I(hk\ell)} = \sum_\alpha \overline{f}_\alpha^2$, where $\overline{f}^2$ is the mean value of the scattering factor in the range of $\sin^2\theta/\lambda^2$ considered. The factor needed to convert the experimental intensity I' to I can be found by dividing the reflections into groups covering the range of $\sin^2\theta/\lambda^2$ and forming the values $\sum \overline{f}^2 / \overline{I'(hk\ell)}$. This value should be a linear function

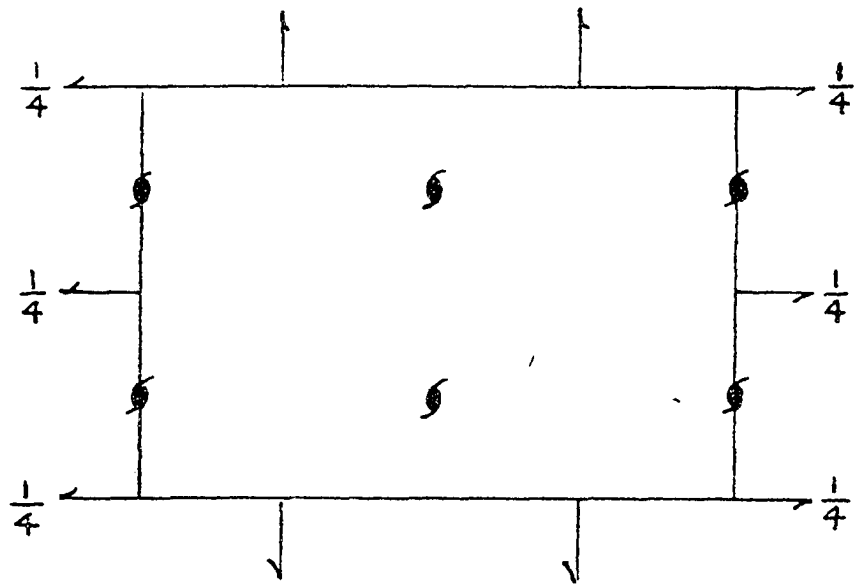

Fig. 1 Symmetry operations in the space group $P2_12_12_1$.

General positions

$x, y, z;$

$\frac{1}{2} - x, \bar{y}, \frac{1}{2} + z;$

$\frac{1}{2} + x, \frac{1}{2} - y, \bar{z};$

$\bar{x}, \frac{1}{2} + y, \frac{1}{2} - z.$

of $\sin^2\theta/\lambda^2$ provided the temperature factor is of the form $\exp(-B \sin^2\theta/\lambda^2)$. Undoubtedly, coincidences in projection must occur for the cyclohexaamylose, tending to make the value of the correction factor too small, but since these coincidences cannot be determined without a knowledge of carbon and oxygen positions, the values of the correction factors are the best approximation that can be made to obtain the absolute scale. Wilson curves for cyclohexaamylose are shown in Fig. 2.

Three-dimensional Patterson Projection

A complete three-dimensional Patterson projection involving approximately 800 independent terms was prepared on IBM using punched cards. This involved the synthesis of sixteen sections at intervals of 2/60 along the x-axis. From the two sections at 0/60 and 30/60 given by the series

$$H(\tfrac{1}{2}yz) = 4\sum_{o}^{\infty}\sum_{o}^{\infty} K(k\ell) \cos 2\pi ky \cos 2\pi \ell z$$

where $K(k\ell) = \sum_{o}^{\infty} (-1)^h F^2(hk\ell)$

and

$$H(0yz) = 4\sum_{o}^{\infty}\sum_{o}^{\infty} K(k\ell) \cos 2\pi ky \cos 2\pi \ell z$$

where $K(k\ell) = \sum_{o}^{\infty} F^2(hk\ell)$

the iodine atoms were located: (Fig. 3)

$x_1 = .250$ $\qquad$ $x_2 = .250$

$y_1 = .153$ $\qquad$ $y_2 = .095$

$z_1 = .500$ $\qquad$ $z_2 = .292$

expressed as fractions of corresponding unit cell dimensions.

Application of Booth's back-correction method (5) resulted in the following iodine positions:

$x_1 = .250$ $\qquad$ $x_2 = .250$

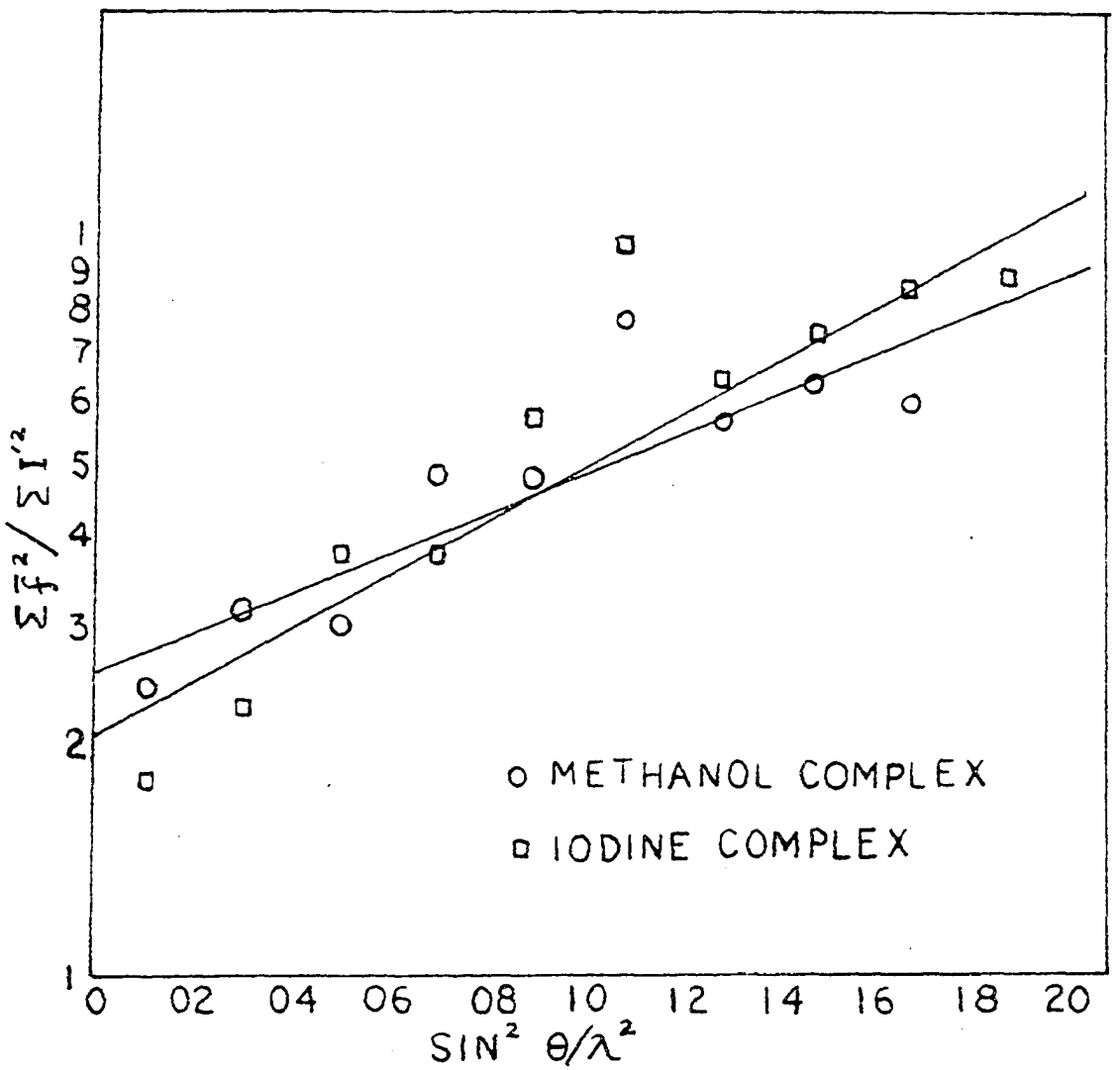

Fig. 2 Wilson curves of the dextrin complexes for (0kℓ) data.

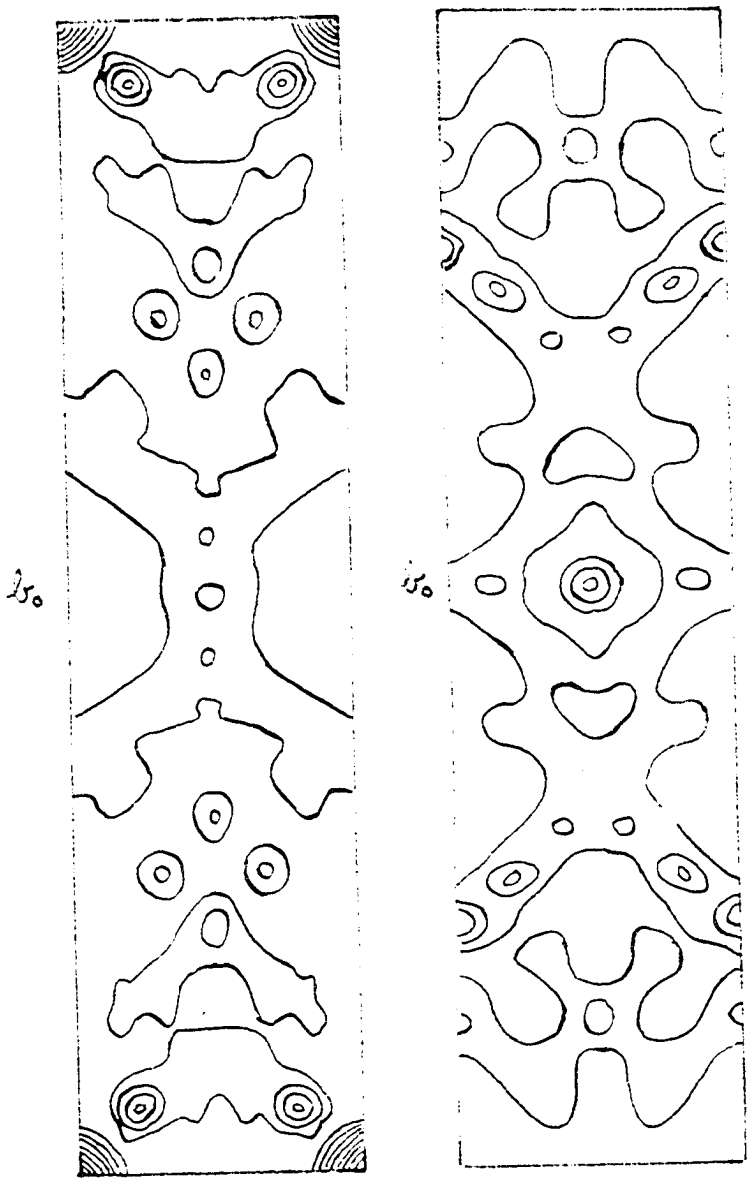

Fig. 3 Harker sections.

$y_1 = .150$ $\qquad$ $y_2 = .095$

$z_1 = .500$ $\qquad$ $z_2 = .292$

expressed as fractions of corresponding unit cell dimensions. The iodine-iodine bond distance is 2.81Å.

From the sixteen Harker sections a plot was made for the section (x,½z,z), (Fig. 4). Unfortunately, the section must, of necessity, include cylinders whose axes are normal to one another, (Fig. 5). But it still gives striking confirmation of the torus-like or cylindrical arrangement of the glucose units surrounding the iodine molecule. The dimensions of the ring are in accord with those previously obtained by methods which are independent of X-ray data.

Fourier Projections

Fourier projections of the iodine complex onto the (001) and (100) planes are shown in Fig. 6.

An electron density map of the carbon and oxygen atoms onto the (100) plane was obtained on X-RAC. The phases and amplitudes were determined from the knowledge of the iodine positions and the isomorphous technique. This necessitated an absolute scale of structure factors. The agreement between the F(0kℓ) of the methanol complex and the F(0kℓ) of the iodine complex after subtracting off the iodine contributions is shown in Table 1.

On this basis of comparison it appears safe to conclude that the absolute scale factor is of a reasonable value.

By means of X-RAC it was possible to make use of the condition of positiveness of the density function (6). The technique as used on X-RAC

Fig. 4 Harker section

(x½zz).

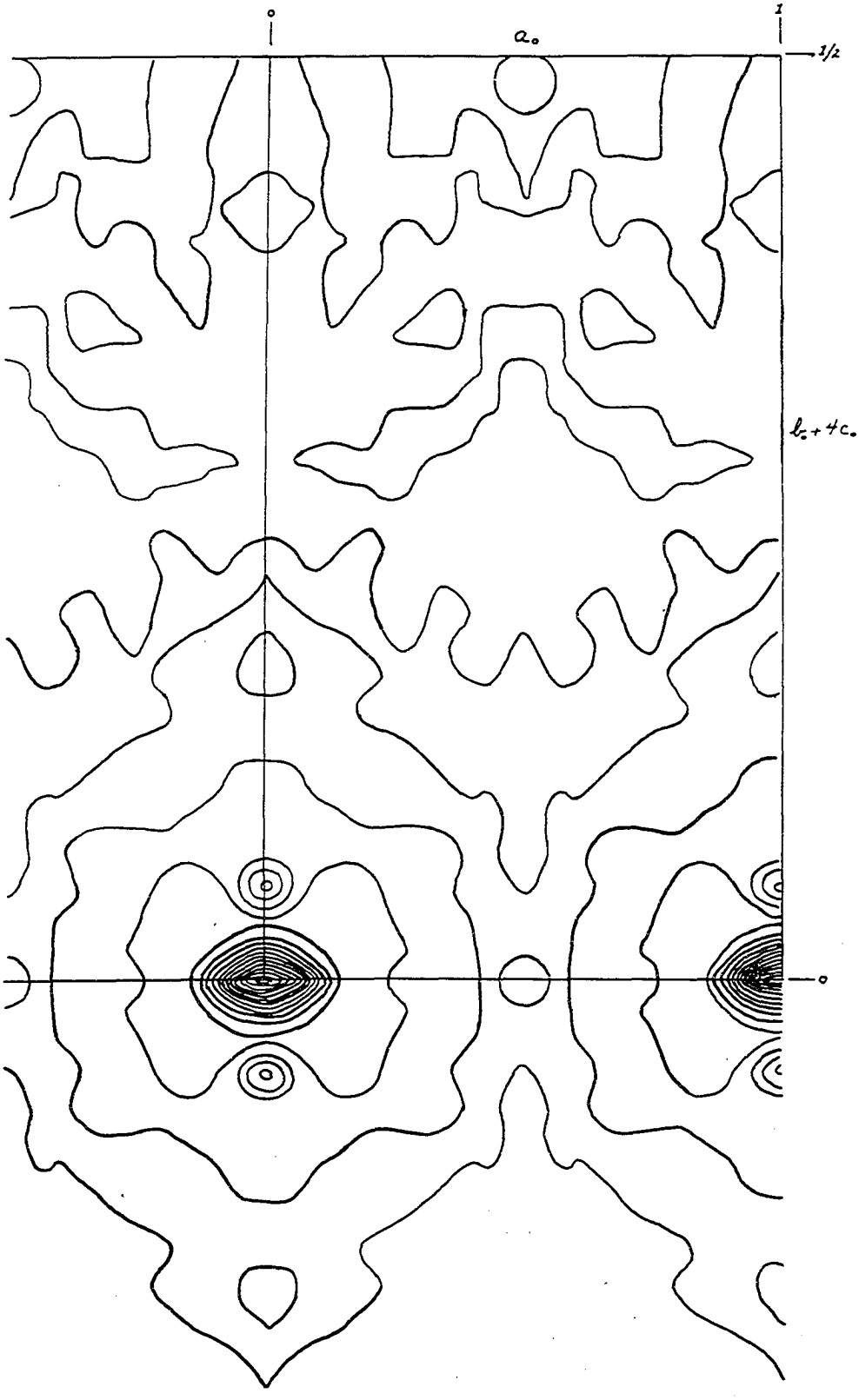
0
a_o
1
1/2
$b_o + 4c_o$
0

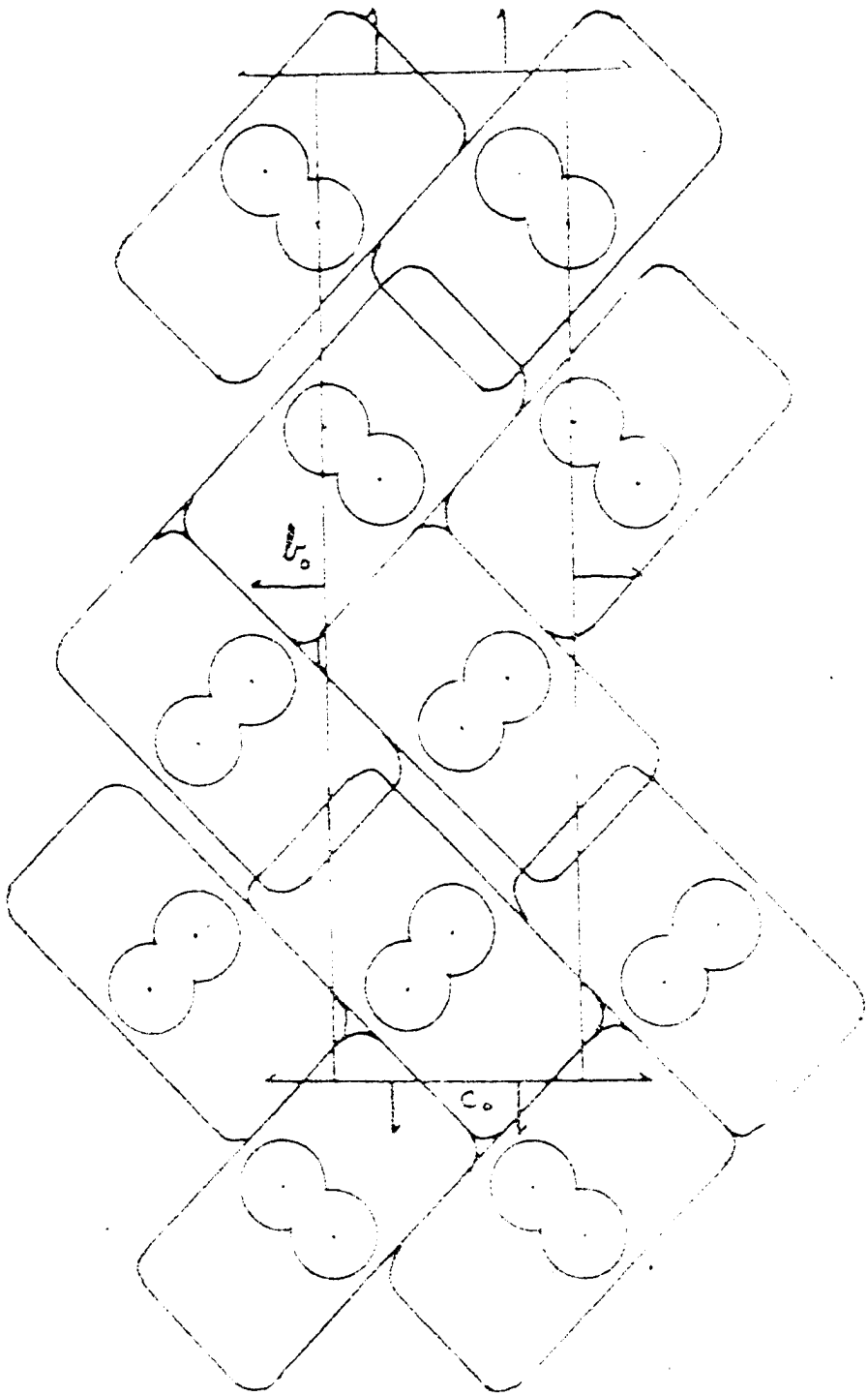

Fig. 5 Projection onto the (100) plane.

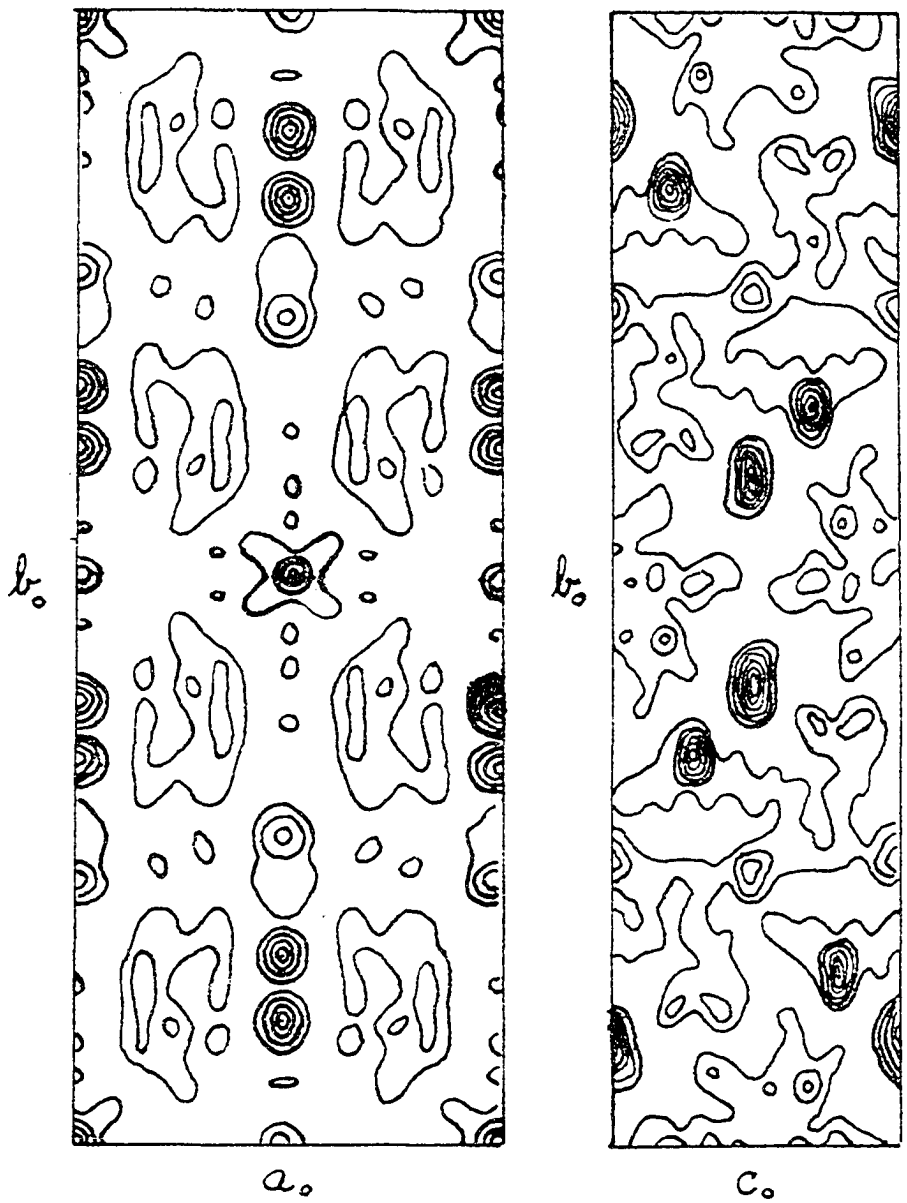

Fig. 6 Fourier projections onto the (001) and (100) planes.

Table 1

Observed and Calculated Structure Factors

Indices	F_o	F_c	Indices	F_o	F_c
	(0kℓ)		(05ℓ)		
(00ℓ)			1	0	+11
2	30	-24	2	118	-160
4	36	-12	3	90	-108
6	34	+100	4	122	-114
			5	0	-68
(01ℓ)			6	0	+25
1	102	+143			
2	94	-106	(06ℓ)		
3	104	+127	0	46	+67
4	64	-53	1	94	-121
5	0	-28	2	208	-198
6	0	-35	3	32	+122
			4	70	-109
(02ℓ)			5	101	+87
0	0	+2	6	0	-95
1	30	+31			
2	96	-119	(07ℓ)		
3	77	-77	1	62	+82
4	126	+151	2	62	-65
5	95	-30	3	104	-107
6	0	-31	4	0	+56
			5	0	+38
(03ℓ)			6	98	-43
1	202	-196			
2	146	+211	(08ℓ)		
3	55	-72	0	138	-94
4	96	+85	1	52	+22
5	0	+26	2	0	+64
6	0	-19	3	36	+4
			4	0	+48
(04ℓ)			5	0	-25
0	70	+46	6	60	-10
1	160	+191			
2	30	-48	(09ℓ)		
3	30	-75	1	142	+172
4	0	+14	2	0	+19
5	0	+19	3	90	-129
6	0	+66	4	36	-160
			5	0	-11
			6	0	+68

Table 1 (Continued)

Indices	F_o	F_c	Indices	F_o	F_c
(0•10•ℓ)			(0•15•ℓ)		
0	142	-127	1	32	+51
1	172	-215	2	0	+63
2	36	-35	3	40	-132
3	92	-29	4	87	-65
4	58	-59	5	0	+66
5	0	+8	6	148	+169
6	0	-35			
			(0•16•ℓ)		
(0•11•ℓ)			0	185	+82
1	148	+138	1	32	+105
2	0	-80	2	208	+141
3	40	+105	3	72	+9
4	62	-97	4	0	+34
5	89	+94	5	0	-2
6	0	+74	6	0	+16
(0•12•ℓ)					
0	164	+138			
1	114	+114			
2	56	-56			
3	42	-16			
4	0	-28			
5	0	+18			
6	0	+62			
(0•13•ℓ)					
1	94	+94			
2	72	-78			
3	30	+3			
4	155	-198			
5	0	-38			
6	0	+95			
(0•14•ℓ)					
0	76	+67			
1	99	-25			
2	0	-44			
3	0	-29			
4	74	-54			
5	0	-19			
6	0	+39			

is to assume that the signs of high amplitudes are correctly determined from the heavy atom parameters, and then to vary the signs of the remaining structure factors, noting the effect on the background.

The application of these methods did not result in any useful information (Fig. 7). It was suggested that three-dimensional electron density maps be prepared, using the phases of the iodine atoms as controlling the signs, but this was set aside in favor of the Fourier transform method (7).

Fourier Transform

The initial attack of the problem involved an integration of the structure factor expression for the space group $P2_12_12_1$ over the limits of a cylindrical shell. An expression was obtained involving the product of two Bessel functions, but the equation for the transform of a cylinder as derived by Wrinch (8) was simpler to evaluate. A brief review of the Fourier transform and its application to distributions in continuous space follows.

The transform of any group of atoms or molecules pictures the contribution of that group to the total scattering power of the crystal, thus permitting the group to be treated as one unit. Obviously the complexity of the problem is reduced by the decrease in the number of parameters. Both Ewald and Patterson have shown that in a crystal structure, a transform reduces to a weighted reciprocal lattice (9). This readily follows if we consider the case of a single atom. The structure factor of the atom referred to its center as origin, the atomic scattering factor, is a function defined at every point of reciprocal space. If now each point

Fig. 7. Fourier projection of oxygen and carbon atoms on the (100) plane.

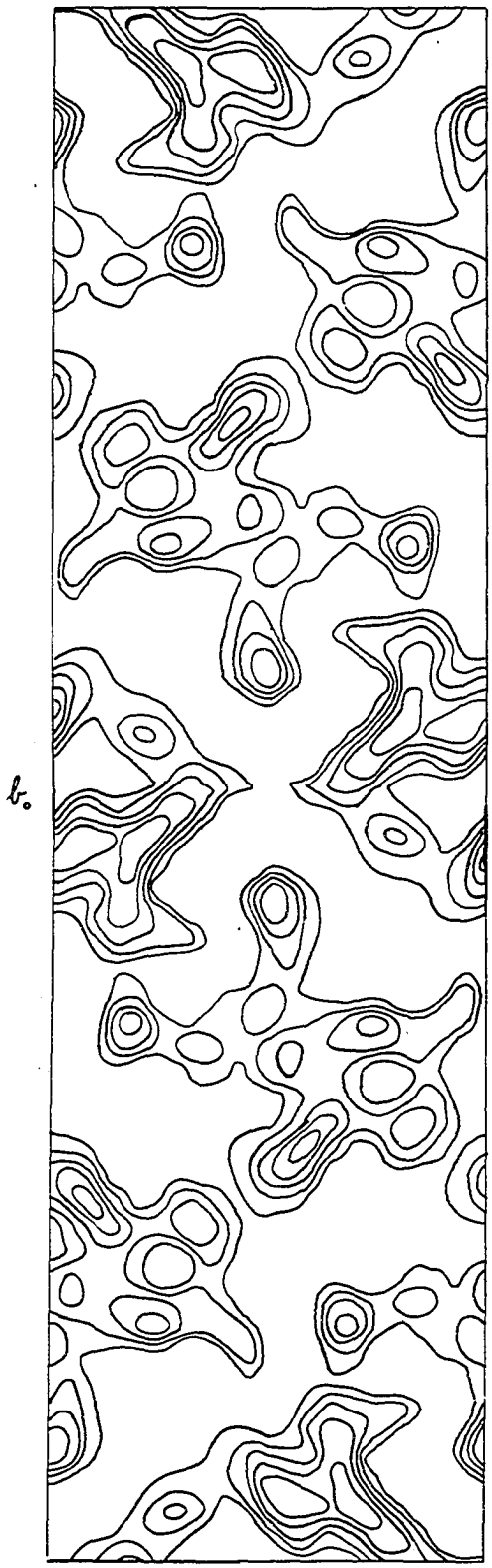
b_o
c_o

is weighted with this function, a representation of the atom throughout reciprocal space is obtained. This method is applicable to any spatial pattern of atoms, as shown by Knott (10). If the distribution function is periodic, its transform can be replaced by Fourier coefficients. From the above definition of the structure factor, it is apparent that the coefficients are identical with Ewald's weighted reciprocal lattice.

We can thus visualize the representation of a distribution by its structure factor as a mapping of the whole of reciprocal space with this function. The map can then be sampled at the reciprocal lattice of any crystal.

In the case of cyclohexaamylose, it is simplest to consider the distribution as a right circular cylindrical shell with a uniform smearing-out of the electron density. Let x, y, and z be referred to orthogonal axes in real space. Using cylindrical coordinates

$$x = r \cos \phi \qquad y = r \sin \phi \qquad z = z$$

and in reciprocal space

$$X = R \cos \Phi \qquad Y = R \sin \Phi \qquad Z = Z$$

the transform may be written thus:

$$wT(R\Phi Z) = \int_{-\infty}^{\infty} \int_{0}^{2\pi} \int_{0}^{\infty} rg(r\phi z) \exp 2\pi i rR \cos(\phi-\Phi) \exp 2\pi i zZ \, dr d\phi dz$$

$$g(r\phi z) = w \int_{-\infty}^{\infty} \int_{0}^{2\pi} \int_{0}^{\infty} RT(R\Phi Z) \exp -2\pi i rR \cos(\phi-\Phi) \exp -2\pi i zZ \, dR d\Phi dZ$$

where T represents the transform of the array and w is the weight. The number of electrons in the distribution is w v and g is the electron distribution function. If the array of atoms has an n-fold symmetry axis and if $g(r\phi z)$ is independent of ϕ, we may write

$$wT(R\Phi Z) = 2\int_{-\infty}^{\infty}\int_{0}^{\infty} rg(rz)\exp 2\pi izZ\left\{\int_{0}^{\pi}\cos\left[2\pi rR\cos(\phi-\Phi)\right]d\phi\right\}drdz$$

$$= 2\pi\int_{-\infty}^{\infty}\int_{0}^{\infty} rg(rz)J_0(2\pi rR)\exp 2\pi izZ\,drdz$$

where $J_0(u)$ is a Bessel function of zero order defined as

$$\pi J_0(u) = \int_{0}^{\pi}\cos(u\cos p)dp$$

Assuming a constant g, the transform of one cylinder may then be expressed as

$$T(R\Phi Z) = 2\pi\int_{x_0}^{x_1}\int_{0}^{Z_1} rJ_0(2\pi rR)\exp 2\pi i\ell z\,drdz$$

where $r = \sqrt{x^2 + y^2}$ and $R = \sqrt{h^2 + k'^2}$. For the two-dimensional case (Okℓ) $R = k'$ where $k'_+ = \sqrt{2}(k+\ell)$ and $k'' = \sqrt{2}(k+\ell)$. Let $2\sqrt{2}\pi(k+\ell)r = x$; then

$$\int \frac{x}{2\sqrt{2}\pi(k+\ell)}\ J_0(x)\ \frac{dx}{2\sqrt{2}\pi(k+\ell)} = \frac{1}{8\pi^2(k+\ell)^2}\int_{x_0 = r_0(2\sqrt{2}\pi(k+\ell))}^{x_1 = r_1(2\sqrt{2}\pi(k+\ell))} xJ_0(x)dx$$

In the limiting case, for $k+\ell = 0$,

$$\frac{1}{8\pi^2\alpha^2}\left[8\pi^2\alpha^2\left(\frac{r_1^2 - r_0^2}{2}\right)\right] = \frac{r_1^2 - r_0^2}{2}$$

The limiting value for the integral is 7.6×10^{-3} where the limits are $x_0 = .267$ and $x_1 = 1.13$.

Since there are four molecules of the dextrin in the unit cell, composed of identical pairs orthogonal to one another (Fig. 5), it is necessary to displace these distributions to a common origin. Since the transform function is independent of the choice of origin for the distribution, we may multiply each independent function by a modulating factor.

Upon shifting the two-fold screw axes to the origin the modulating factors become

$$M_1 = \cos 2\pi \left[k(0.372) + \ell(0.395)\right]$$
$$M_2 = \cos 2\pi \left[k(0.628) + \ell(0.605)\right]$$
$$M_3 = \cos 2\pi \left[k(0.872) + \ell(0.105)\right]$$
$$M_4 = \cos 2\pi \left[k(0.128) + \ell(0.895)\right]$$

The expression for the total transform is

$$T = 2(M_1 + M_3)\left\{\frac{1}{4\ell}\left|\sin 2\pi\ell\,(.250)\right|\frac{1}{8\pi^2(k+\ell)^2}\int_{x_o}^{x_1} xJ_o(x)\,dx\right\}$$

Values of T for $k + \ell$ from zero to ten were calculated. These were compared with the signs and amplitudes of the structure factors obtained from the isomorphous methanol complex to evaluate the feasibility of the transform approach. The integrals involving the product $xJ_o(x)$ were obtained by use of Simpson's rule. The subdivisions were chosen on the basis of least error in the maximum value of $k + \ell$.

DISCUSSION

Density Maps

It is difficult to explain the failure of the electron density projections onto the (100) plane to give information concerning the more exact location of the carbon and oxygen atoms. The agreement between the experimental data from the two isomorphous compounds is at odds with the results.

The factor that might well obscure the finer detailing of the dextrin structure may be the high degree of hydration. There are between twelve and fourteen waters of hydration to each molecule of dextrin.

The Fourier Transform Technique

The values of the structure factors obtained by this technique fall off much more rapidly than would be expected from the cylindrical transform. A $g(r,z)$ increasing to a maximum in the central regions of the cylindrical shell and falling off to a minimum at the edges, such as a Gaussian curve, might prove more favorable to the electron distribution existing.

It would be well to consider the effect of varying the limits upon the magnitudes and signs of the structure factors. The limits are by no means well defined and at higher values of $k + \ell$, the magnitudes and signs of the structure factors are sensitive to the position of the boundaries.

In the transform approach, the water of hydration is not considered, since it is believed that the water packs in holes between the tori. This

might also account for the poor agreement obtained on the low order reflections.

It appears that the above facts should be taken into careful consideration before the applicability of the transform technique can be rightly evaluated.

Further Studies

The study of both cyclic and linear dextrins suitable for crystal structure analysis may prove profitable if continued. The ability of the non-reducing dextrins to form crystalline complexes of many modifications when reacted with iodine in the presence of iodide ion justifies a detailed study of their crystal classes and unit cell sizes. Chemical and physical studies of many of the complexes of cyclohexaamylose have been made by French (11).

Hexaamylose and heptaamylose have been prepared from acid hydrolysis of the corresponding cycloamyloses (12). Such compounds, particularly the latter, should prove most valuable in establishing the physical configuration of the starch chain. However, all attempts to crystallize these compounds up to the present time have failed.

The hydrolysis of the γ-dextrin (octaamylose) should proceed at a greater rate than the α- and β-dextrins and give fewer degradation products. Due to its larger size and the fact that higher amyloses such as decaamylose can be crystallized, it should not be unreasonable to expect crystallization. In addition, there is evidence that dextrins containing an even number of glucose units crystallize more readily (13).

SUMMARY

Crystals of cyclohexaamylose from 50 per cent aqueous propanol, ethanol, and methanol are nearly isomorphous with the cyclohexaamylose-iodine complex. The unit cells are orthorhombic with the space group D_2^4—$P2_12_12_1$ and contain four molecules.

The iodine parameters are $x_1 = .250$, $y_1 = .150$, $z_1 = .500$, $x_2 = .250$, $y_2 = .095$, $z_2 = .292$ expressed as fractions of the corresponding unit cell dimensions. The iodine molecules lie in the (100) plane at an angle of 45° to the major axes. The iodine-iodine bond distance is 2.81Å.

A complete three-dimensional Patterson confirms the torus-like arrangement of glucose units coaxial with and surrounding each iodine molecule. The size of the torus is in agreement with dimensions obtained by methods independent from X-ray techniques.

The Fourier transform technique is not successful in locating carbon and oxygen atoms.

The results of the three-dimensional analysis lend further support to the existence of a helical configuration in the amylose-iodine complex.

PART II.

STRUCTURE OF

TETRAMETHYLAMMONIUM ENNEAIODIDE

INTRODUCTION

Studies of the chemical and physical behavior of the polyhalogen compounds have resulted in many interesting observations for which satisfactory answers are still being sought. Why is the ease of crystallization and the stability of the polyhalides a function of the size and nature of the cation present? Do the polyhalides make use of the d-orbitals above the valence shell in bonding, as do polyhalogens composed of two or more different halogens? Are linear trihalides of only one halogen unsymmetrical as reported by some investigators?

It is with the view to answering these questions or verifying the conclusions reached by others that the author has undertaken this study to elucidate the physical configuration of tetramethylammonium enneaiodide.

REVIEW OF THE LITERATURE

Probably most prominent among the early workers in polyhalide chemistry was A. Geuther who prepared crystalline salts of the type MI_{2n-1} with n ranging in value from one to four (14). Geuther made the interesting observation that the stability of the polyiodides was a function of the size of the cation present and that the higher species did not occur unless the cation was as large or larger than the tetramethylammonium ion.

Ludecke in conjunction with Geuther carried out optical studies on several of the polyiodides. He reported crystals of $N(CH_3)_4I_5$ to be monoclinic with axial ratios 0.9866 : 1 : 0.6553 and $\beta = 72^\circ\ 20'$ (15). The pleochroic properties of $N(CH_3)_4I_9$ were also reported in the same paper.

Higher polyhalides cannot be prepared with lighter halogens whereas polyhalogens IX_{2n-1} form higher members only when X is fluorine (14). When iodine is substituted for any one or more halogens, the stability of the polyhalogen is increased. This stability appears to be a function of the weight of the halogens present. The following order is observed among the trihalides: $I_3^- > IBr_2^- > ICl_2^- > IBrCl^- > Br_3^-$ $I_2Br^- > I_2Cl^- > Br_2Cl^-$ (16).

In the early 1900's Dawson completed a study of iodide ions in solution and concluded that the I_3^- and I_9^- ions were the lower and upper limits respectively of the polyhalides (17). The experimental evidence also led him to propose the presence of I_5^- and I_7^- ions in solution. Evidence has also been found by Dodson for the presence of X_3^- and X_5^- ions in solution where X may contain as many as three different halogens per ion (18). More recent work by Buckles and Popov using ultraviolet

absorption of $(C_4H_9)_4NBr_3$ in bromotrichloromethane indicates the existence of higher bromides in solution to be dubious (19).

Polyhalides IX^-_{n-2}, where I constitutes the central atom of the ion, have undergone x-ray structural studies by Wyckoff; but by far the most extensive work has been by Mooney on the compounds $N(CH_3)_4I_3$, $N(CH_3)_4ICl_2$, $NH_4IClIBr$, $KICl_4$, and NH_4I_3 (20). The bonding in all but the triiodide is generally assumed to be covalent with the bond lengths closely approximating the sums of the covalent radii and the central iodine atom making use of d-orbitals above the valence shell for bonding. In the ICl^-_4 complex, the central atom is in the center of a square of chlorine atoms. Since two d-orbitals are available for combination with s and p, hybridization of the type sp^3d^2 can occur. The regular octahedron may be then formed by placing each of two unshared electron pairs of iodine above and below the ICl_4 plane (21). Similarly, the configuration of linear ions, IX^-_2, can be interpreted as arising from sp^3d hybridization by placing the two halogens at the apices of a trigonal bypyramid and the three unshared electron pairs in the equatorial plane (21).

However, the reported structure of the triiodide ion shows an asymmetric linear ion with iodine distances of 2.82 and 3.10Å, longer than found in I_2 (22). The investigation was made at a time when methods of refinement were somewhat limited and some doubt was cast upon the accuracy of the reported distances.

Because of the questionable accuracy of these I-I bonds, Hach and Rundle carried out the structure determination of $N(CH_3)_4I_5$ (23). Iodine-iodine distances within one net were sufficiently different to justify

singling out V-shaped I_5^- ions with iodine distances 2.93 and 3.14Å. The bonding in the I_5^- ion differed from that found in Mooney's ICl_4^-. The authors interpret the bonding without the use of d-orbitals above the valence shell. The polyiodide ions arise as a result of interaction of the iodide ion with highly polarizable I_2 molecules. Resonance of the various forms of the ions lend stability to the structure. As the cation becomes smaller, the resonating form with the negative charge closest to the positive charge predominates resulting in a progressively longer iodine-iodine bond. The resulting decrease in resonance stabilization is offered as an explanation of why the higher polyiodides occur only when the cation is large.

EXPERIMENTAL

Preparation and Analysis

Crystals of the compound and analysis data were obtained by R. Hach (24). The crystals were prepared from an ethanol solution of tetramethylammonium iodide containing a two- or three-fold excess of iodine. The crystals possess a greenish-black metallic luster and on exposure to air slowly lose iodine, which deposits on the surface.

Samples were analyzed for iodide by volatilizing free iodine at about 200°C. The average of three samplings was 16.53 per cent as compared to the theoretical value of 16.53 per cent. The observed density obtained using a pycnometer with mineral oil was 3.47 gm/cc as against a calculated density of 3.51 gm/cc obtained from X-ray data.

Diffraction Data

A crystal of nearly rectangular cross section and edges of 0.015 and 0.030 cm ± 10 per cent was inserted into a thin-wall glass capillary (24). X-ray data using CuKα radiation normal to the needle axis of the crystal was obtained. Lattice level symmetry of Weissenberg photographs placed the crystal in the monoclinic class. A primitive lattice was indicated by reflections from all types of planes. The (h0ℓ) reflections were observed only when $\ell = 2n$. The (0k0) reflections were present only when $k = 2n$. The space group was accordingly $P2_1/c$.

Oscillation pictures about the needle axis coupled with a zero level Weissenberg pattern were used to obtain the lattice constants and the β

angle. The values are as follows:

$$a_o = 13.16\text{Å}$$
$$b_o = 15.10 \qquad \beta = 136^\circ\ 35'$$
$$c_o = 16.69$$

The inconvenience of working with such a large angle suggested a reselection of the a_o and c_o axes to give a β of $95^\circ\ 25'$. The (h0ℓ) reflections now appear only when $h + \ell = 2n$, resulting in the space group $P2_1/n$.

The final lattice constants were obtained from precession data. The camera was calibrated by means of a calcite crystal. The lattice constants are:

$$a_o = 11.60\text{Å}$$
$$b_o = 15.10 \qquad \beta = 95^\circ\ 25'$$
$$c_o = 13.18$$

The space group contains 4 $N(CH_3)_4I_9$/unit cell. Symmetry operations of the space group $P2_1/n$ are shown in Fig. 8.

Precession photographs timed to give a film factor of two were taken about the needle axis using MoKα radiation. Data of the type (h0ℓ), (0kℓ), (hk0), (hkh), and (hk$\bar{h}$) were obtained. The intensities were obtained by visual comparison methods and corrected for Lorentz and polarization factors to give relative F^2's.

Patterson Projections

Patterson projections utilizing (h0ℓ), (hk0), and (0kℓ) precession data were synthesized on IBM using punched cards. These are shown in Fig. 9, 10, and 11.

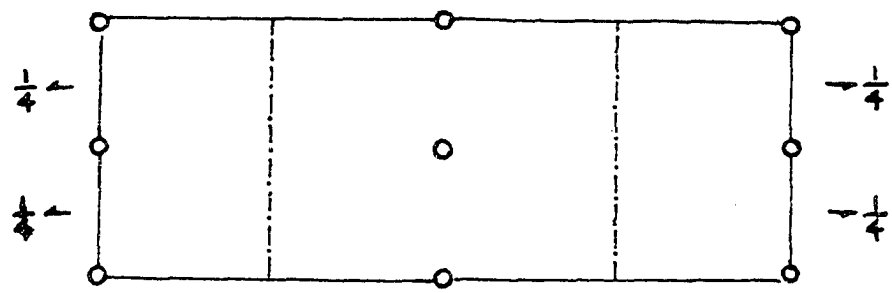

Fig. 8 Symmetry operations in the space group $P2_1/n$.

Point positions	Structure factor
2: (a) (000, $\frac{1}{2}\frac{1}{2}\frac{1}{2}$)	$h + k + \ell = 2n$
(b) (00$\frac{1}{2}$, $\frac{1}{2}\frac{1}{2}$0)	$A = 4 \cos 2\pi(hx + \ell z)\cos 2\pi ky$
(c) (0$\frac{1}{2}$0, $\frac{1}{2}$0$\frac{1}{2}$)	$B = 0$
(d) ($\frac{1}{2}$00, 0$\frac{1}{2}\frac{1}{2}$)	$h + k + \ell = 2n + 1$
4: (e) xyz; $\frac{1}{2}+x$, $\frac{1}{2}-y$, $\frac{1}{2}+z$;	$A = -4 \sin 2\pi(hx + \ell z)\sin 2\pi ky$
$\overline{xyz}$; $\frac{1}{2}-x$, $\frac{1}{2}+y$, $\frac{1}{2}-z$.	$B = 0$

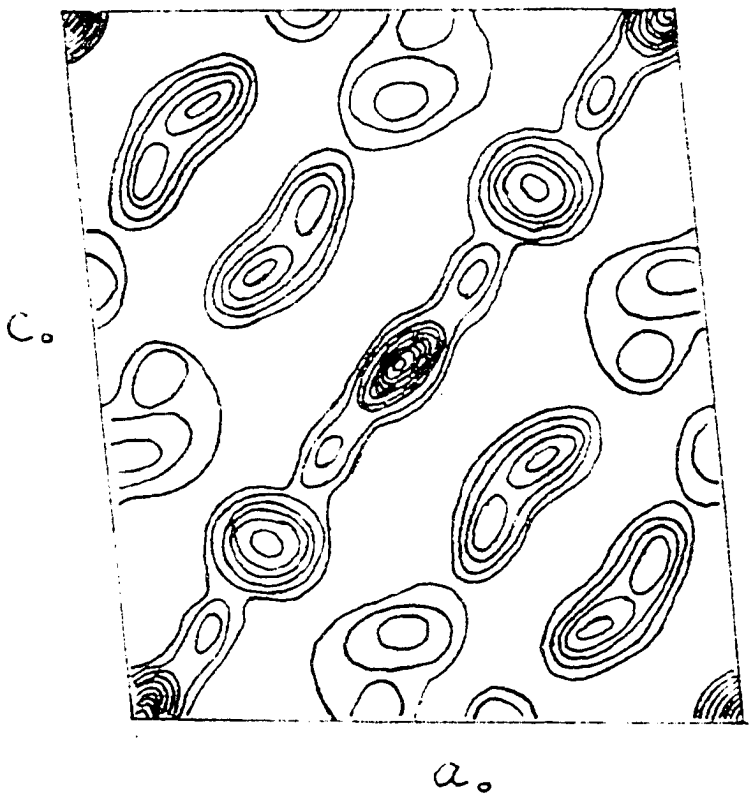

Fig. 9 Patterson projection down b_o.

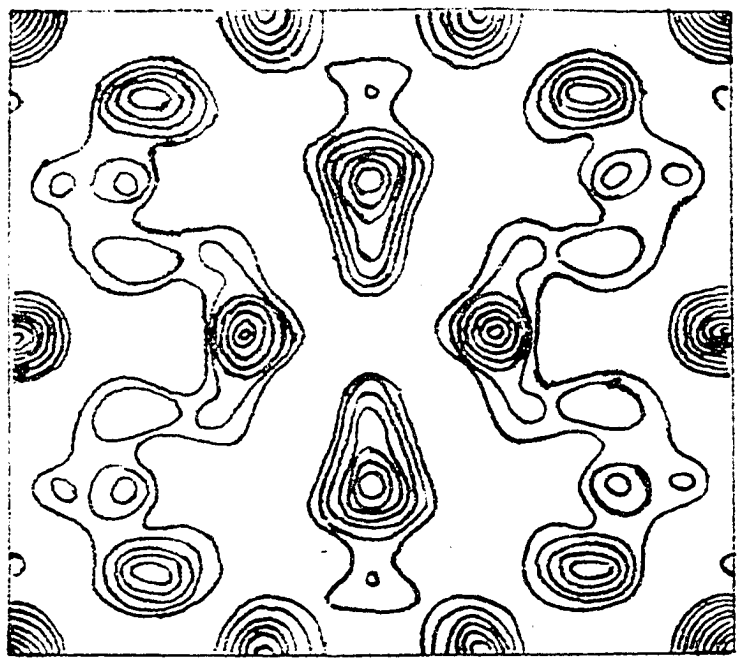

Fig. 10 Patterson projection down a_o.

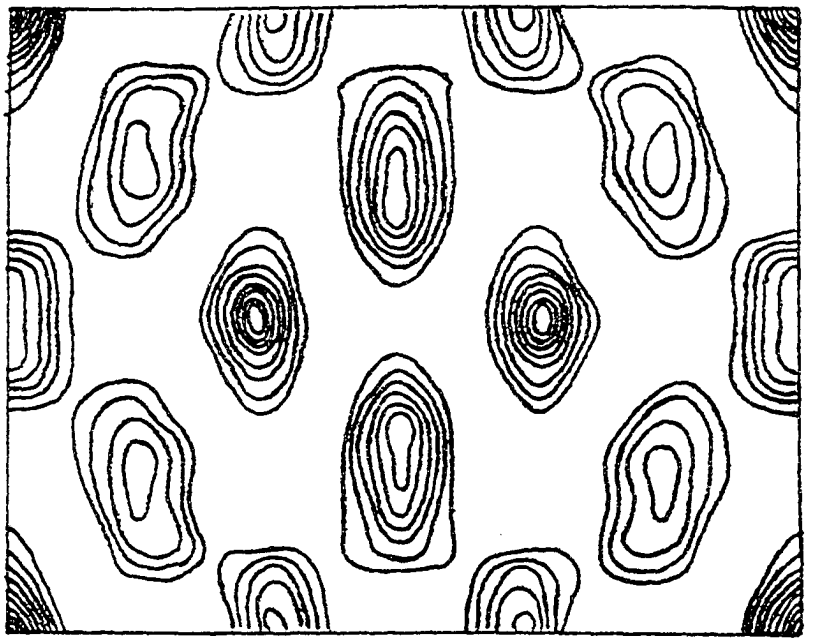

Fig. 11 Patterson projection down c_o.

The projection onto the (010) plane indicated that all the iodine atoms project into lines in the direction of $a_o - c_o$. Accordingly vector maps were prepared from (hkh) and (hk$\bar{h}$) precession data and are shown in Fig. 12 and 13.

Fourier Projection

Using trial and error procedures and the restrictions placed upon the possible interpretations of the (010) Patterson, Hach obtained the electron density map shown in Fig. 14.

A study by Hach of this Fourier synthesis suggested that three iodine atoms coincided in projection at x = 42/60 and z = 10/60 of the respective axial lengths (Fig. 14). It will be noted that the peaks are nicely defined and that the electron densities are those expected for three atoms in one peak and two in the remaining. In addition the peaks are elongated in the direction of $a_o - c_o$ suggesting that the iodine atoms do not project directly onto one another.

The reliability factor $R = \frac{\sum \left| |F_o| - |F_c| \right|}{\sum |F_o|}$ calculated for this interpretation was 0.29.

Determination of y Parameters

Hach then proceeded to make Fourier maps from eight trial structures considered to be the only eight possible in an attempt to determine the y parameters. These attempts failed to give any satisfactory results. The failure to obtain agreement between observed and calculated structure factors involving the y parameters led Hach to suggest that the (010) Fourier

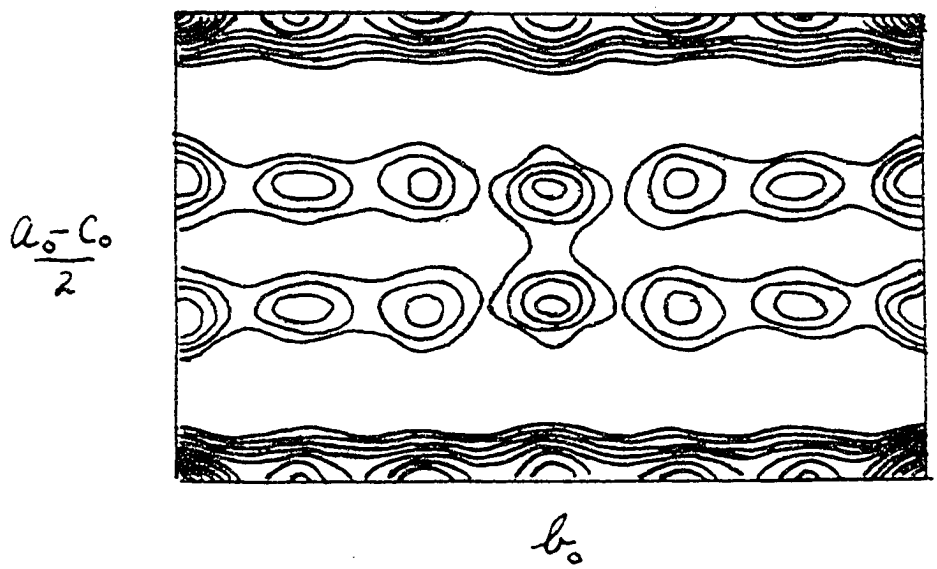

Fig. 12 Patterson projection down $a_o - c_o$.

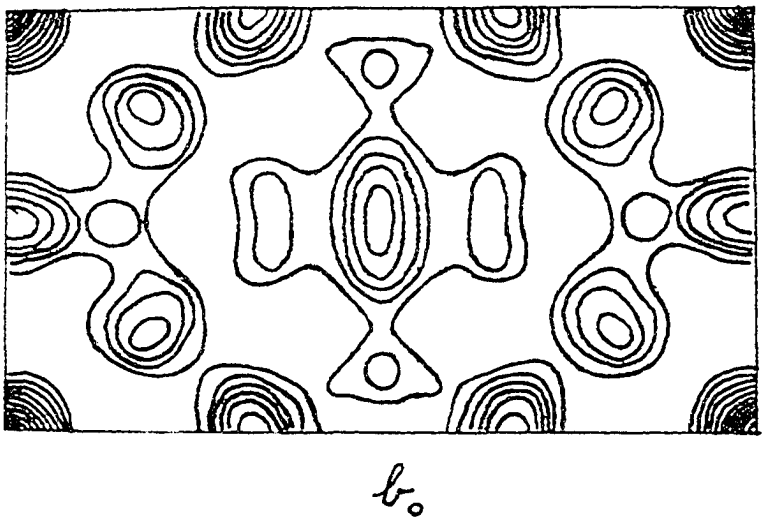

Fig. 13 Patterson projection down $a_o - c_o$.

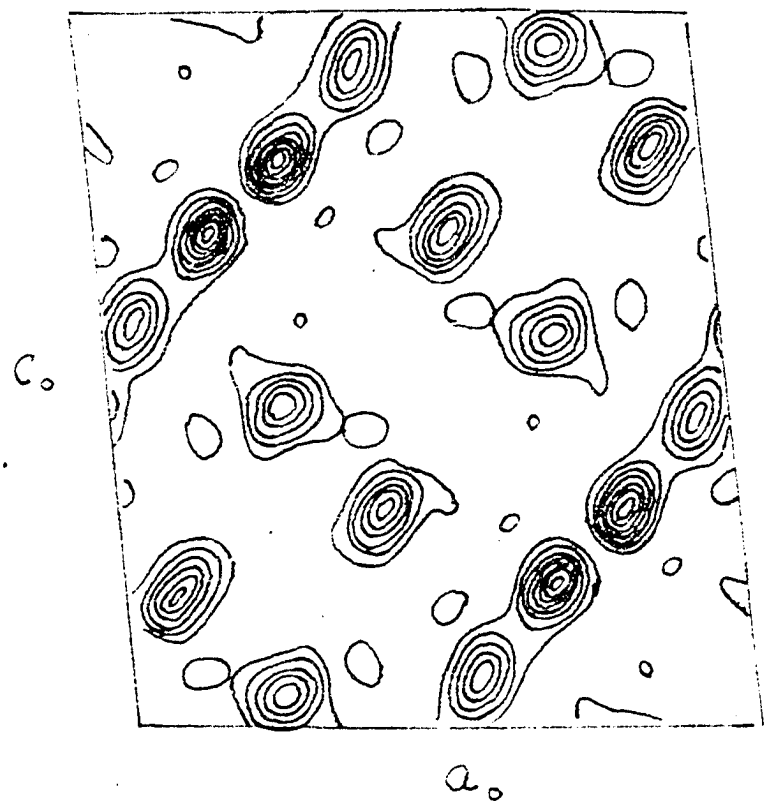

Fig. 14 Fourier projection onto the (010) plane.

was in error, and that this would most readily be ascertained by a refinement of the x and z parameters.

However, in the light of the fact that the intensity data for this plane were of doubtful accuracy and because of the high degree of overlap, this author felt that some method independent of refinement and trial and error techniques should be sought.

A careful study of the eight possible trial structures was made by superposing two-dimensional projections of the suggested models onto their corresponding vector maps. It appeared that none of the combinations of y parameters suggested in the eight structures was correct. However, the analysis of the Fourier map onto (010) appeared compatible with the corresponding Patterson projection with one major exception. The peaks occurring at x = 4/60, z = 4/60, x = 8/60, z = 13/60 did not possess the heights dictated by the vectors arising from the presence of three atoms at x = 42/60, z = 10/60 and two atoms at the remaining sites. The multiplicities are such that both peaks should be of approximately equal heights (Fig. 9).

Sharpened Patterson

Accordingly a sharpened Patterson onto (010) was prepared (Fig. 15). There are several methods for increasing the resolution of Patterson distributions (25). As will be noted from the Patterson projections shown, the maxima are rather diffuse resulting from the rapid diminution of the coefficients. If coefficients were chosen which did not decrease at all with $\sin^2\theta$, this would correspond physically to point atoms resulting in

Fig. 15 Sharpened Patterson onto the (010) plane.

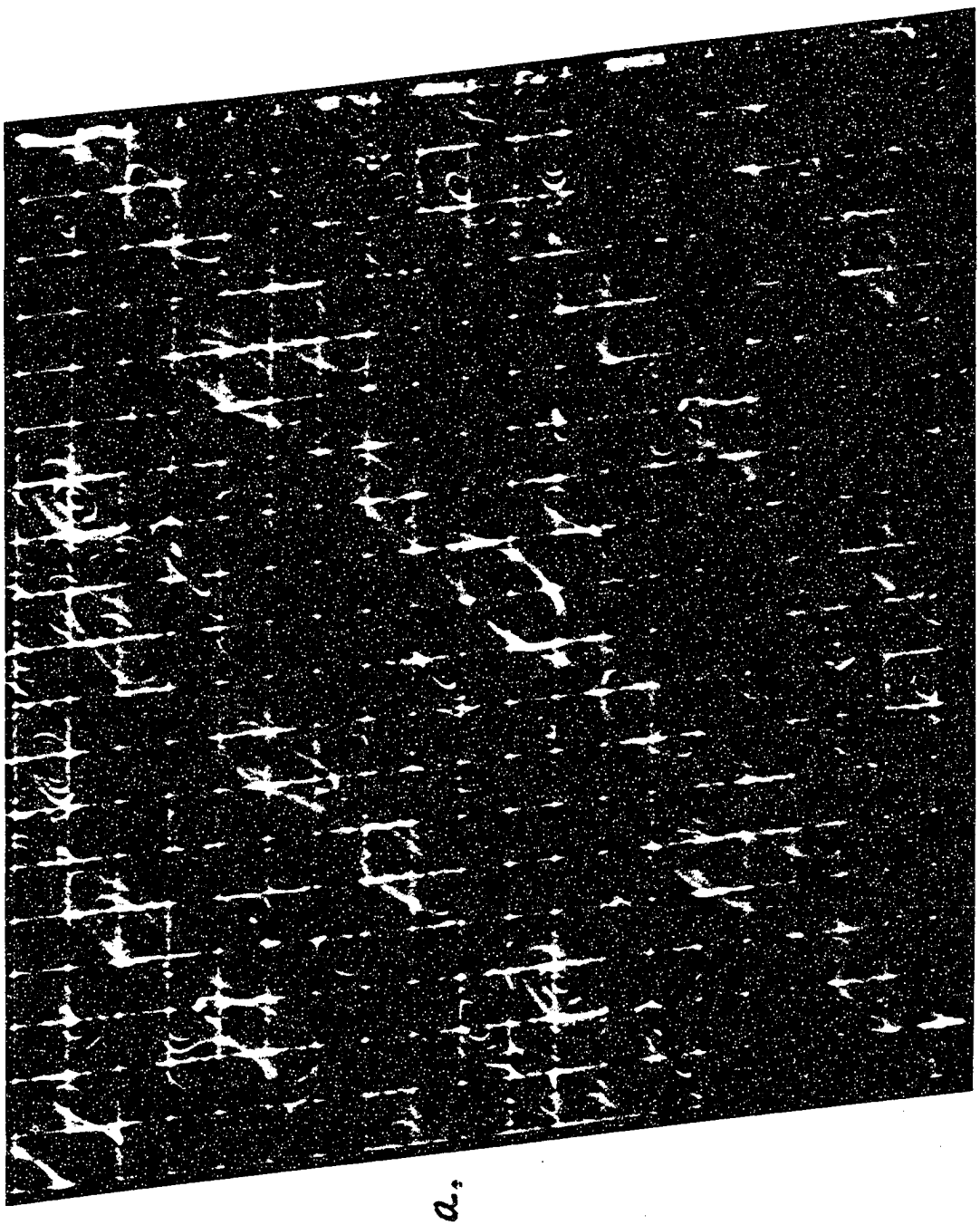

a_0

c_0

sharpened maxima. As a consequence, however, many false peaks would occur due to termination of the series at a finite number of terms.

The use of a temperature factor is suggested as a means of reducing the rate at which the coefficients diminish. Therefore, the relative values of the structure amplitudes squared were placed on an absolute scale using the method of A. J. C. Wilson previously described. The presence of a large number of atoms of the same scattering power occupying general positions lends itself well to this statistical procedure. Wilson curves are shown in Fig. 16.

Only three-fourths of the observed temperature factor was applied to the observed intensities in order to lessen the effect of series termination. The results of the sharpened Patterson were to verify the conclusions reached by Hach, Fig. 15.

Inequalities

The main difficulty encountered in structural study is the fact that measurements are made of $|F_{hk\ell}|$ rather than $F_{hk\ell}$. The solution of the phase problem has received considerable attention in recent years; and prominent among the suggested solutions from the viewpoint of successful application is the method of mathematical inequalities.

In order that the reader may better appreciate the application of this technique to the work here reported, a condensed review of the method in its various modifications follows.

The first important and practical contribution may be considered that of Harker and Kasper (26). Their procedure gains in applicability through

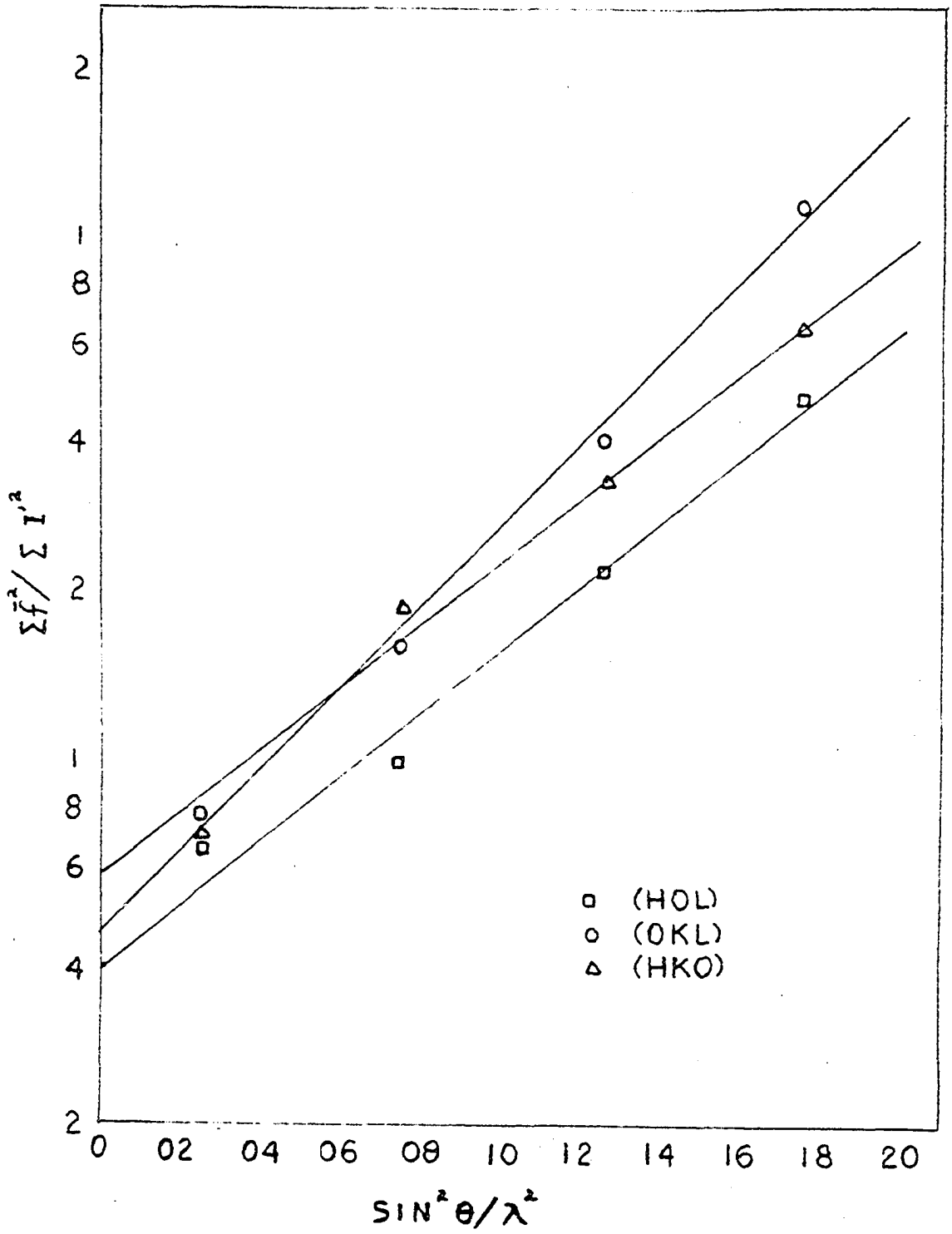

Fig. 16 Wilson curves.

its introduction of unitary structure factors. These are calculated in a manner similar to a method used for sharpening Patterson distributions. A reasonable approximation is the assumption that the atom scattering factors f_j of the atoms in a crystal are related by the expression $f_j = Z_j f$, where Z_j is the atomic number of the jth atom and f is the unitary scattering factor.

$$\text{If } Z = \sum_{j=1}^{N} Z_j \text{ , then } \sum_{j=1}^{N} f_j = Zf.$$

Substitution of the expression for f_j into the structure factor expression enables one to write

$$U_{hk\ell} = \sum_{j=1}^{N} n_j \exp 2\pi i(hx_j + ky_j + \ell z_j)$$

where $U_{hk\ell} = F_{hk\ell}/Zf$ (unitary structure factor) and $n_j = Z_j/Z$. By application of Cauchy's inequality to the above expression and the assumption of a center of symmetry, the following relation is derived

$$U^2_{hk\ell} \leq \tfrac{1}{2} - \tfrac{1}{2}U_{2h2k2\ell} \cdot$$

Inequalities of the same general form are obtained on application of other elements of symmetry. Thus for any space group a large number of inequalities of increasing complexity may be derived.

One of the undesirable features of the above is the increasing complexity of the expressions as symmetry elements are combined. The work of Grison (27) has resulted in expressions more suitable for experimental application. From the most powerful inequality relation deduced by Harker and Kasper, $|U_H \pm U_{H'}| \leq (1 \pm U_{H+H'})(1 \pm U_{H-H'})$ where H and H' refer to the indexes of the reflections, Grison derived the relationships shown in Table 2.

Table 2

Grison Relationships

Equations	If	Conditions
$A = (1+ \lvert U_{H+H'} \rvert)(1+ \lvert U_{H-H'} \rvert)$	E>B>D>F	$S_H S_{H'} = S_{H+H'} = S_{H-H'}$
$B = (1+ \lvert U_{H+H'} \rvert)(1- \lvert U_{H-H'} \rvert)$	E>B>F>D	Incompatible
$C = (1- \lvert U_{H+H'} \rvert)(1+ \lvert U_{H-H'} \rvert)$	E>C>D>F	$S_H S_{H'} S_{H+H'} = +$
$D = (1- \lvert U_{H+H'} \rvert)(1- \lvert U_{H-H'} \rvert)$	E>C>F>D	$S_H S_{H'} S_{H+H'} = +$ and $S_H S_{H'} S_{H-H'} = -$
$E = (\lvert U_H \rvert + \lvert U_{H'} \rvert)^2$	E>F>C>D	Incompatible
$F = (\lvert U_H \rvert - \lvert U_{H'} \rvert)^2$	E>D>F	$S_{H+H'} S_{H-H'} = -$ or $S_H S_{H'} S_{H+H'} = +$
where $\lvert U_{H+H'} \rvert > \lvert U_{H-H'} \rvert$	E>F>D	$S_{H+H'} S_{H-H'} = -$

The limitations of the method of inequalities have been published by Hughes (28). A standard for evaluating the feasibility of the inequalities approach is given by the root-mean-square value σ of the unitary structure factors. The σ value is defined by

$$\sigma^2 = \sum_{j=1}^{N} n_j^2 \quad \text{where} \quad n_j = f_j \Big/ \sum_{1}^{N} f_j$$

or, for a primitive unit cell containing N atoms of the same scattering power, by the relation $\sigma = 1/\sqrt{N}$. With decreasing σ, a large fraction of the amplitudes will have magnitudes too small to permit the determination of their phases.

The work of Zachariasen, Sayre, and Cochran (29), (30), (31) was an attempt to extend the method of inequalities to more complex structures

involving lower σ values, i.e., a small percentage of large unitary structure factors. Along very different paths, these authors ended up with the same conclusion, namely the probable validity of the relation $S_{H+K} = S_H \cdot S_K$, where S denotes the algebraic signs of three strong reflections. The method of Harker and Kasper assures the validity of this equation, provided the signs can be determined. Frequently, however, few such equations can be obtained if few atoms add in phase. It has been shown by Zachariasen that the method of inequalities as introduced by Harker and Kasper will lead to a structure determination if 20 percent or more of the structure factors satisfy the condition $|U_H| > 0.30$. This implies a $\sigma > 0.22$. Therefore, one can only take recourse in a procedure which is not necessarily, but probably, correct. This method is a very useful analytical tool which reduces to a problem of self-consistency with respect to the relationships between signs. When coupled with chemical intuition, the dangers of such an analytical process are diminished.

Results of Inequalities

The methods of Grison were applied to (h0ℓ) data. Since the contribution to scattering is predominately of iodine, the unitary structure factor can be written as

$$U_{hk\ell} = \frac{|F_{hk\ell}|}{N f_{hk\ell}} .$$

A total of 59 out of 79 observed reflections were obtained. (Table 3). A Fourier projection (010) was synthesized on X-RAC. The results were almost identical with the electron density map obtained by Hach.

Having established the validity of Hach's density map, it was decided that this approach should be applied to other two-dimensional data to

Table 3

Unitary Factors and Signs

Indices	U(h0ℓ)	Sign		U(h0ℓ)	Sign
(h00)					
4	.10	+	1	.41	+
8	.36	−	3	.47	+
			5	.15	−
(h01)					
$\bar{7}$	.46	−	(h06)		
$\bar{5}$	.15	+	$\bar{8}$	.22	−
3	.21	−	$\bar{6}$	.52	+
5	.24	−	$\bar{4}$	.37	−
7	.25	+	$\bar{2}$	.35	+
9	.15	+	0	.13	+
11	.40	−	2	.34	−
(h02)			(h07)		
$\bar{10}$	.41	−	$\bar{9}$	.38	−
$\bar{8}$	.24	+	$\bar{7}$	.29	−
$\bar{6}$	.25	+	$\bar{5}$	.65	+
$\bar{4}$	.37	+			
$\bar{2}$	.33	+	(h08)		
2	.44	−	$\bar{8}$	.39	+
4	.19	+	$\bar{4}$	.24	−
6	.33	−	0	.66	−
8	.12	+			
			(h09)		
(h03)			$\bar{7}$	.72	+
$\bar{5}$	.15	+	$\bar{5}$	.31	−
$\bar{3}$	.71	−	$\bar{3}$	.32	−
1	.25	−			
5	.46	+	(h010)		
7	.17	+	$\bar{8}$	.75	−
			$\bar{4}$	.36	−
(h04)			2	.25	+
$\bar{10}$	.60	+			
$\bar{6}$	.15	+	(h011)		
$\bar{4}$	.21	+	$\bar{5}$	.40	+
$\bar{2}$	.34	−	$\bar{3}$	.39	+
0	.09	+			
2	.13	+	(h012)		
8	.31	+	$\bar{6}$	.49	+
			$\bar{2}$	.38	+
(h05)					
$\bar{7}$	.52	−			
$\bar{5}$	.55	−			

obtain information on the y parameters. Because the atoms overlapped to a lesser degree on the other planes, a lower σ value was obtained. Due to the corresponding decrease in the fraction of larger amplitudes, it was necessary to apply the self-consistent technique previously mentioned. This was done by plotting the (0kℓ) and (hk0) reflections on a grid (Fig. 17). For convenience, only unitary factors of 0.25 were chosen. Since the space group is centrosymmetric, the signs of two reflections may be chosen at will, provided they are not independent of the choice of origin. For example, the sign of an (0k0) reflection or an (0kℓ) reflection where $k = 2n$, $\ell = 2n$ could not be chosen arbitrarily. The origin of the graph corresponds to a unitary structure factor of one with a positive sign. The application of a self-consistent relationship between signs consists of observing the signs of all vectors between reflections related to the same chosen reflection. For example, if the sign of the (023) reflection were positive, then all vectors where $\Delta k = 2$, $\Delta \ell = 3$ should be positive. As more terms of lower magnitudes were introduced upon the grid, some inconsistencies arose. The phases of these lower amplitudes were determined by the predominence of one sign among the vectors.

A Fourier projection down a_o was prepared for approximately 27 reflections on X-RAC (Fig. 18). The phases of those weaker amplitudes which were questionable were determined through use of the positivity criteria (6). Although the projection was originally misleading, the information thereon together with scalar model studies was instrumental in solution of the final structure.

The application of inequalities to the (hk0) data did not result in any useful information although a considerable degree of consistency was

Fig. 17 Grid of the (Okl) reflections.

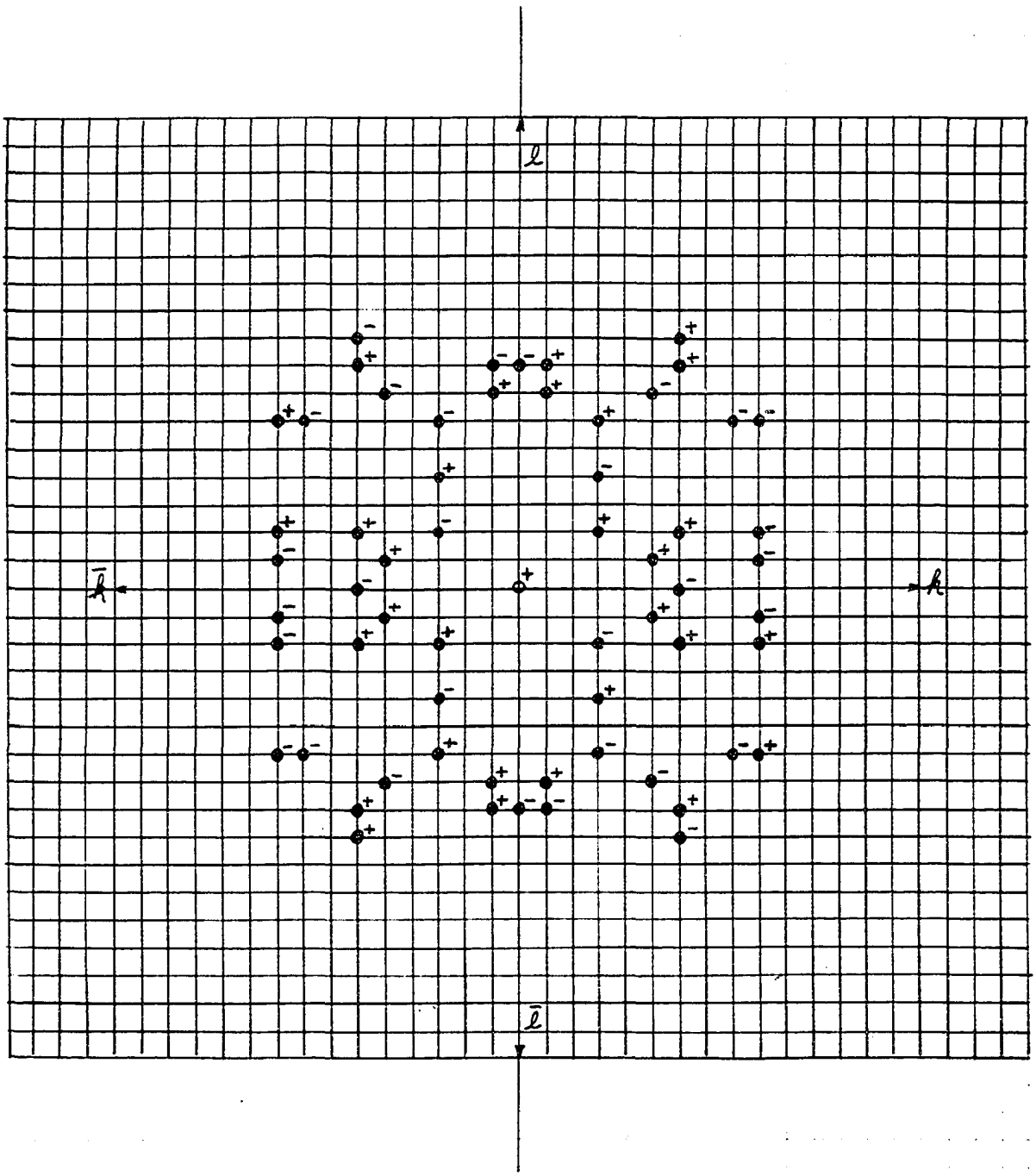
l
$\bar{h}$
h
$\bar{l}$

Fig. 18 Fourier projection down a_o.

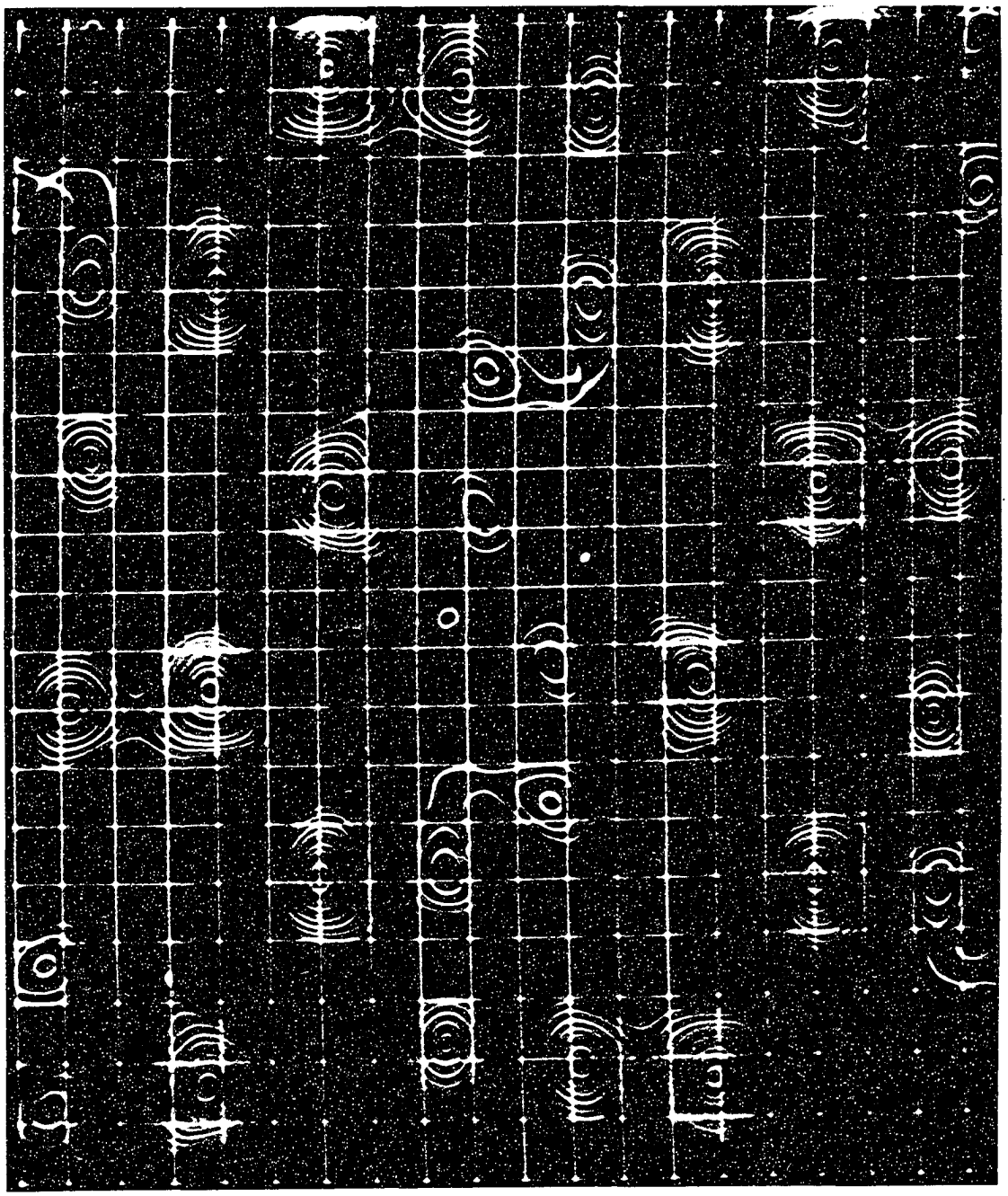
c°
b°

obtained between signs of the structure factors. Presumably a few signs of some larger amplitudes were in error. As previously noted the method does not assure the validity of the phases.

Refinement of the Parameters

The use of the synthetic Fourier with backshift corrections, although used extensively for the refinement of parameters, is not well suited to refinement when atoms overlap in projection. The difference synthesis technique developed by Cochran (32) and used by Finbak (33) is better applied in this situation. The approach might be considered an outgrowth of Booth's steepest descents (34) involving primarily the minimization of the function $R = \sum w(|F_o| - |F_c|)$ with respect to atomic coordinates, where w is a weighting factor involving the error in the estimation of intensities. A plot of $\rho_o - \rho_c$ is made assuming that the signs of the calculated structure factors for the larger amplitudes are correct. After the synthesis is complete, the positions of the atoms are compared with those used for calculating the structure factors. For example, if the atomic coordinates were very much in error, a large negative or positive peak corresponding to a too great or a too small electron density would occur at that point. For smaller errors the centers of the peaks would be shifted somewhat. Corrections to the parameters are made in the direction of greatest initial slope. This procedure is repeated until the reliability factor R is minimized.

The difference synthesis is said to be equivalent to the normal Fourier method plus the Booth correction or stated otherwise the rate of convergence is approximately equal to that of least squares (35).

Difference syntheses of the series

$$D = \rho_o - \rho_c = \sum_{hk\ell} (F_o - F_c) \cos 2\pi(hx+ky+\ell z)$$

were synthesized for both (0kℓ) and (hk0) data (Fig. 19 and 20). Successive maps were made and the reliability factor R determined after each correction to the parameters. These refinements were carried out until the change in R was negligible. In addition the parameters obtained from these two planes were used to calculate R factors for (h0ℓ) and (hkh) data. The final values of the parameters are listed in Table 4. The R factors for observed (h0ℓ), (0kℓ), (hk0), and (hkh) data are, respectively, 0.17, 0.18, 0.17 and 0.16. The agreement between calculated and observed structure factors are shown in Table 5. Fourier maps for (0kℓ) and (hk0) data were synthesized from the final parameters and are shown in Fig. 21 and 22.

Fig. 19 Difference synthesis of (0kℓ) data.

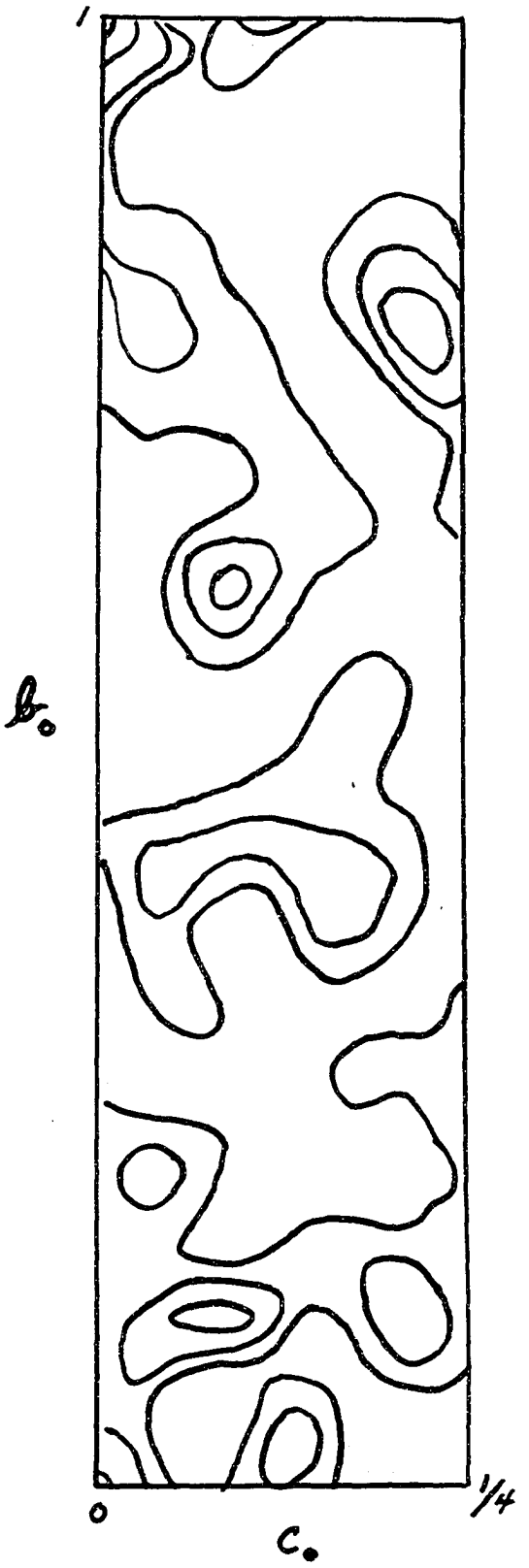
1
b.
0
1/4
c.

Fig. 20 Difference synthesis of (hk0) data.


1
b_o
0
a_o
1/4

Table 4

Parameters of the Iodine Atoms

X	Y	Z
$X_1 = .211$	$Y_1 = .058$	$Z_1 = .041$
$X_2 = .076$	$Y_2 = .084$	$Z_2 = .190$
$X_3 = .046$	$Y_3 = .880$	$Z_3 = .586$
$X_4 = .086$	$Y_4 = .416$	$Z_4 = .189$
$X_5 = .041$	$Y_5 = .318$	$Z_5 = .534$
$X_6 = .249$	$Y_6 = .400$	$Z_6 = .061$
$X_7 = .181$	$Y_7 = .084$	$Z_7 = .690$
$X_8 = .191$	$Y_8 = .729$	$Z_8 = .710$
$X_9 = .150$	$Y_9 = .455$	$Z_9 = .665$

Table 5

Observed and Calculated Structure Factors

Indices	F_o	F_c	Indices	F_o	F_c
	(hk0)				
(0k0)					
2	140	+146	2	114	+102
4	152	-151	3	0	+16
6	238	-235	4	22	+3
8	67	-76	5	10	+12
10	32	+30	6	60	+83
12	12	+16	7	0	+19
14	20	-14	8	39	+29
			9	32	+47
(1k0)			10	36	-13
3	0	+2	11	67	-60
4	14	-7			
5	172	-158	(4k0)		
6	58	-69	0	49	+56
7	33	+35	1	70	-66
8	53	+44	2	68	-63
9	68	+75	3	123	+128
10	0	+8	4	62	-55
11	14	+6	5	14	+3
12	20	+35	6	14	+14
13	0	-1	7	14	+7
14	28	-18	8	28	+31
			9	32	+39
(2k0)			10	51	+33
0	48	-58	11	14	+15
1	57	-79			
2	56	-56	(5k0)		
3	309	-270	1	98	+84
4	74	-73	2	127	+100
5	135	-127	3	69	+52
6	109	+102	4	39	-52
7	72	-59	5	82	-82
8	0	-3	6	62	-73
9	68	+85	7	0	-26
10	0	+22	8	47	-56
11	28	+40	9	20	-44
12	14	+10	10	6	-8
			11	0	+6
(3k0)					
1	33	-20	(6k0)		
			0	41	-40

Table 5 (Continued)

Indices	F_o	F_c
1	0	+3
2	51	-33
3	23	-32
4	69	+76
5	0	0
6	35	+44
7	40	-41
8	0	-3
9	40	+49
10	27	-33
11	17	+24
(7k0)		
1	73	-70
2	14	-14
3	20	-30
4	74	-59
5	53	+39
6	14	+17
7	0	-9
8	41	+51
9	10	-19
(8k0)		
0	99	-89
1	0	+1
2	0	+9
3	49	+59
4	0	+6
5	0	+9
6	25	+35
7	33	-24
8	0	+13
(9k0)		
1	14	-3
2	74	+72
3	10	+12
4	14	+19
5	30	+36
6	14	+10
7	0	-5
8	28	-21

Indices	F_o	F_c
(10k0)		
0	10	-13
1	0	+7
2	0	-4
3	40	+38
4	27	+24
5	7	+9
6	10	-17
(00ℓ)	(0kℓ)	
2	30	-38
4	37	+41
6	45	+57
8	150	-140
10	22	+13
12	14	-14
(01ℓ)		
2	76	+87
3	44	+31
4	0	+9
5	79	+57
6	87	+76
7	85	+64
8	94	+73
9	0	-12
10	0	-10
11	35	-22
12	0	+11
13	0	-3
14	14	-7
(02ℓ)		
0	140	+146
1	0	-5
2	0	-19
3	128	+108
4	66	-60
5	14	+24
6	76	+52
7	0	+2
8	43	-46

Table 5 (Continued)

Indices	F_o	F_c	Indices	F_o	F_c
9	26	+30	8	30	+24
10	0	-8	9	0	-10
11	0	+1	10	14	-25
12	14	+10			
13	14	+10	(06ℓ)		
			0	209	-206
(03ℓ)			1	0	+2
1	37	+23	2	109	+92
2	268	+227	3	45	+33
3	41	-50	4	0	-10
4	198	-181	5	0	-2
5	64	-50	6	14	-22
6	172	+161	7	74	+71
7	0	0	8	77	+78
8	14	17	9	50	+31
9	0	-16	10	28	-20
10	0	-18			
11	20	+15	(07ℓ)		
12	0	+12	1	31	-45
13	0	+11	2	39	+35
14	20	-22	3	0	-15
			4	36	+35
(04ℓ)			5	0	-5
0	143	-141	6	0	0
1	22	+21	7	14	+9
2	46	-61	8	14	+15
3	41	-20	9	20	-9
4	41	+25	10	25	+14
5	43	-35			
6	45	32	(08ℓ)		
7	22	-13	0	48	-54
8	58	+45	1	72	+69
9	0	+7	2	0	-9
10	0	-7	3	0	-5
11	0	-6	4	17	-27
12	14	-7	5	14	-9
			6	73	-55
(05ℓ)			7	0	+37
1	167	+140	8	0	+12
2	127	+122	9	0	-7
3	0	-10	10	14	+15
4	14	-8			
5	0	+6	(09ℓ)		
6	0	+5	1	76	-81
7	72	-54	2	69	-70

Table 5 (Continued)

Indices	F_o	F_c
3	0	-25
4	0	+25
5	26	+22
6	61	-61
7	0	+2
8	14	+6
9	28	+22
10	28	+8
(0·10·ℓ)		
0	27	+25
1	0	+11
2	0	-2
3	42	+20
4	14	+4
5	14	-15
6	28	-17
7	0	-8
8	20	-18
9	0	-14
(0·11·ℓ)		
1	20	-18
2	20	-22
3	33	+34
4	0	+2
5	25	-21
6	0	-8
(0·12·ℓ)		
0	14	+18
1	0	+9
2	14	-21
3	0	-16
4	14	+12
5	0	-3
6	0	+12
(0·13·ℓ)		
1	0	-1
2	14	+16
3	0	+6
4	14	-6
5	0	-11
6	20	+5
(0·14·ℓ)		
0	14	-10
1	32	-24
2	14	-13
3	14	-10
(hOℓ)		
(00ℓ)		
2	20	-25
4	32	+34
6	40	+51
8	121	-113
10	10	+12
($\bar{1}$0ℓ)		
1	120	-116
3	40	+37
5	148	+121
7	14	+14
9	0	-17
(10ℓ)		
1	0	13
3	120	-116
5	20	-30
7	14	-14
9	0	+16
($\bar{2}$0ℓ)		
2	155	+170
4	136	-128
6	105	+111
8	17	+29
10	0	-1
12	32	+37
(20ℓ)		
0	30	-36
2	222	-168
4	49	+73
6	100	-100
8	0	+13
10	35	+43

Table 5 (Continued)

Indices	F_o	F_c	Indices	F_o	F_c
$(\bar{3}0\ell)$					
1	14	+15	$(\bar{6}0\ell)$		
3	285	-293	2	64	+68
5	0	-19	4	36	+35
7	0	+10	6	102	+86
9	50	-44	8	17	+16
11	39	+37	10	0	+13
(30ℓ)			(60ℓ)		
1	92	-87	0	28	-27
3	17	+18	2	86	-81
5	150	+166	4	10	-37
7	14	-16	6	30	-31
9	25	+40	8	14	+21
$(\bar{4}0\ell)$			$(\bar{7}0\ell)$		
2	138	+125	1	101	-111
4	67	+70	3	0	+12
6	91	+79	5	89	-73
8	41	-15	7	37	-43
10	43	-32	9	67	+50
12	0	0			
			(70ℓ)		
(40ℓ)			1	57	+55
0	33	+37	3	33	+46
2	72	+98	5	0	-9
4	25	-12	7	10	+25
6	27	-44	9	0	0
8	0	0			
10	0	-7	$(\bar{8}0\ell)$		
			2	40	+41
$(\bar{5}0\ell)$			4	14	+2
1	51	+60	6	26	-35
3	46	+65	8	33	+32
5	133	-116			
7	117	+94	(80ℓ)		
9	39	-32	0	65	-58
11	33	-28	2	20	+24
			4	46	-29
(50ℓ)			6	0	+4
1	78	-98	8	0	+8
3	137	+164			
5	36	-39	$(\bar{9}0\ell)$		
7	0	-13	1	10	+22
9	0	-11	3	0	+7

Table 5 (Continued)

Indices	F_o	F_c	Indices	F_o	F_c
5	0	+16	2	218	-206
7	32	-30	3	268	+274
			4	63	+77
(90ℓ)			5	0	+19
1	25	+51	6	211	+261
3	0	-8	7	93	-70
5	0	-2	8	39	+44
			9	28	-18
($\overline{10}$•0•ℓ)			10	14	-3
2	39	-37	11	10	+11
4	50	+52			
6	0	-1	(3k3)		
			0	33	+18
(10•0•ℓ)			1	52	+68
0	10	-11	2	0	0
2	0	-9	3	143	+168
			4	89	-90
($\overline{11}$•0•ℓ)			5	17	+27
1	0	+2	6	10	-18
			7	22	-18
(11•0•ℓ)			8	41	+37
1	33	+22	9	68	-81
			10	33	+29
	(hkh)				
(0k0)			(4k4)		
4	159	-151	0	30	-15
6	238	-235	1	137	-124
8	64	-76	2	64	+70
10	32	+30	3	58	-72
			4	36	+5
(1k1)			5	26	-40
2	0	+10	6	0	-20
3	212	-172	7	10	+4
4	118	+118	8	45	-47
5	42	-52	9	33	+25
6	71	-65	10	22	-13
7	115	+129			
8	0	+5	(5k5)		
9	14	+40	0	45	-47
10	22	-29	1	0	-9
11	20	+11	2	0	0
			3	41	-65
(2k2)			4	0	+15
0	234	-235	5	64	-73
1	28	+27	6	64	+70

Table 5 (Continued)

Indices	F_o	F_c
7	0	+2
8	0	+10
9	20	+22
10	25	-22
(6k6)		
0	44	-49
1	0	+8
2	28	+44
3	10	+10
4	30	-9
5	30	+35
6	0	-3
7	0	0
8	0	+1

Fig. 21 Fourier down a_o.

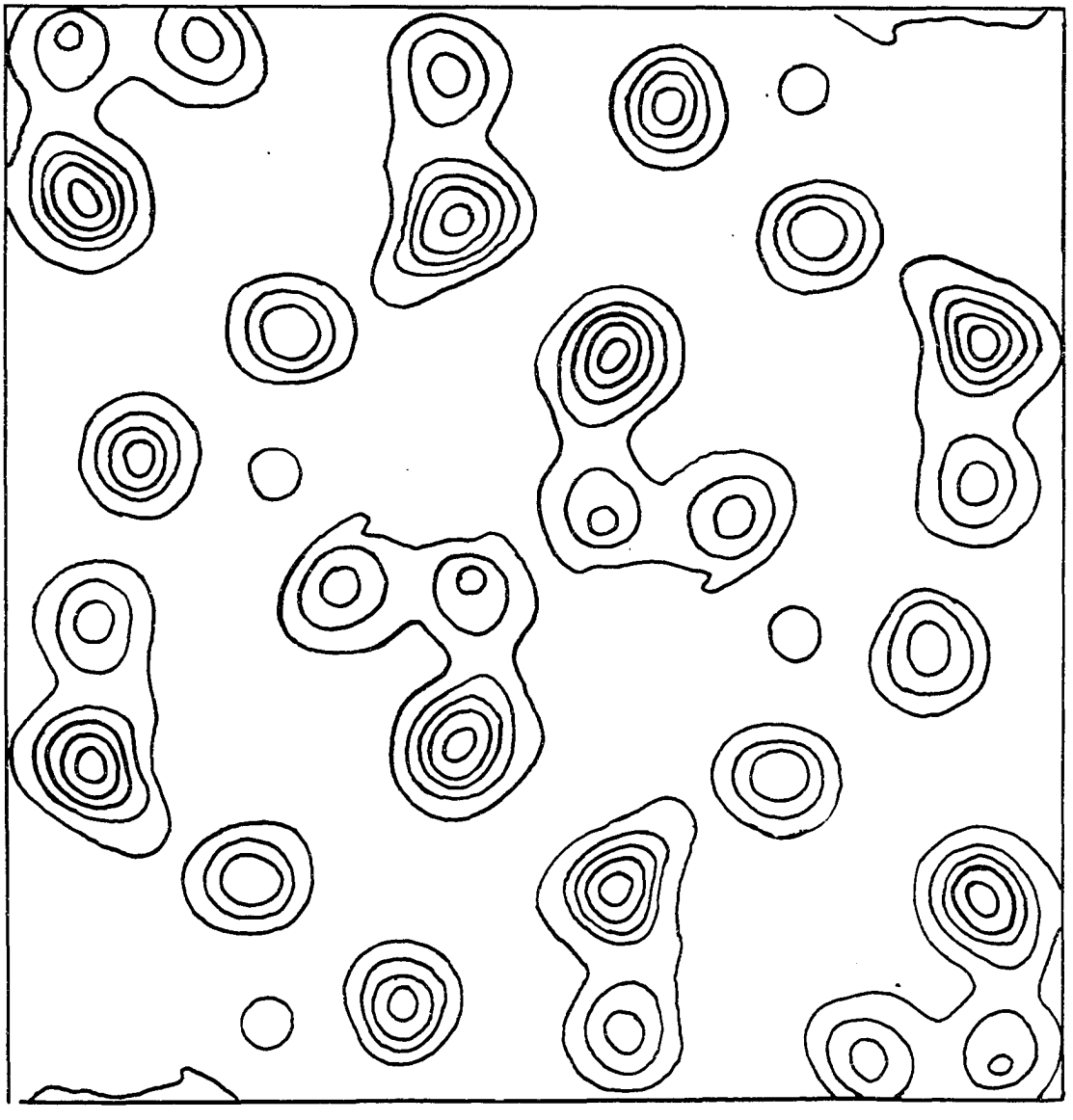
C_o
b_o

Fig. 22 Fourier down c_o.

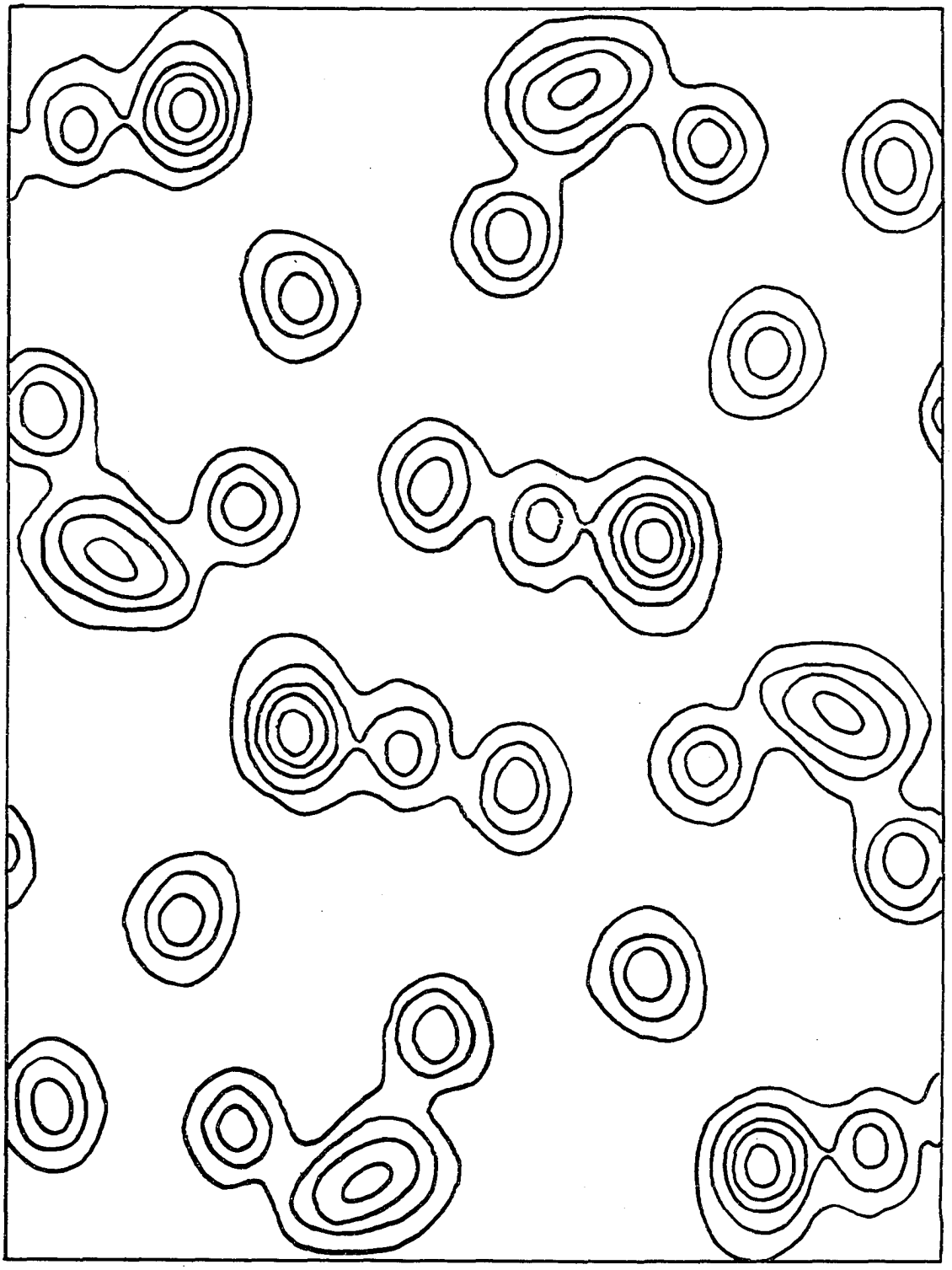
b₀
a₀

DISCUSSION

Description of the Structure

The structure of $N(CH_3)_4I_9$ is shown in Figs. 23, 24, 25, and 26. The enneaiodide structure consists of alternately, nets of iodine molecules packed with the cation and nets of pentaiodide ions. Apparently two iodine molecules and a pentaiodide ion account for the nine iodine atoms of the molecular formula. However, the refinement process has not eliminated alternate interpretations in light of hepta- or enneaiodide ions.

Fig. 24 is a projection of one I_5^- net down the a_o-c_o axes. These iodine atoms lie essentially in planes with a departure from planarity of only $\pm$ 0.20Å. The planes containing the I_5^- ions are separated by a distance of approximately 9.2Å. The separation of I_5^- ions within one plane is shown in Fig. 24. The pentaiodide is V-shaped with an angle of 86.5° at the apex. The arms of the V are linear within approximately 7 degrees. The iodine-iodine bond distances are 3.17Å and 2.90Å in one arm and 2.91Å and 3.24Å in the other.

In Fig. 25, the projection of the I_2 molecules onto the net shown in Fig. 24 suggests a honeycomb arrangement of iodine molecules. The dotted circles represent iodine molecules approximately normal to and behind the plane of anions while the solid circles represent iodine molecules in front of the plane of anions. The iodine atom of the I_2 molecule directly behind the terminal atom of the pentaiodide ion (labeled 3 according to the parameters given in Table 4) is at a distance of 3.43Å. However, the distance to the nearest iodine atom of the I_2 molecule in front of the plane is 3.24Å. It is very doubtful that this latter distance is significant since there

Fig. 23 Structure of $N(CH_3)_4I_9$.

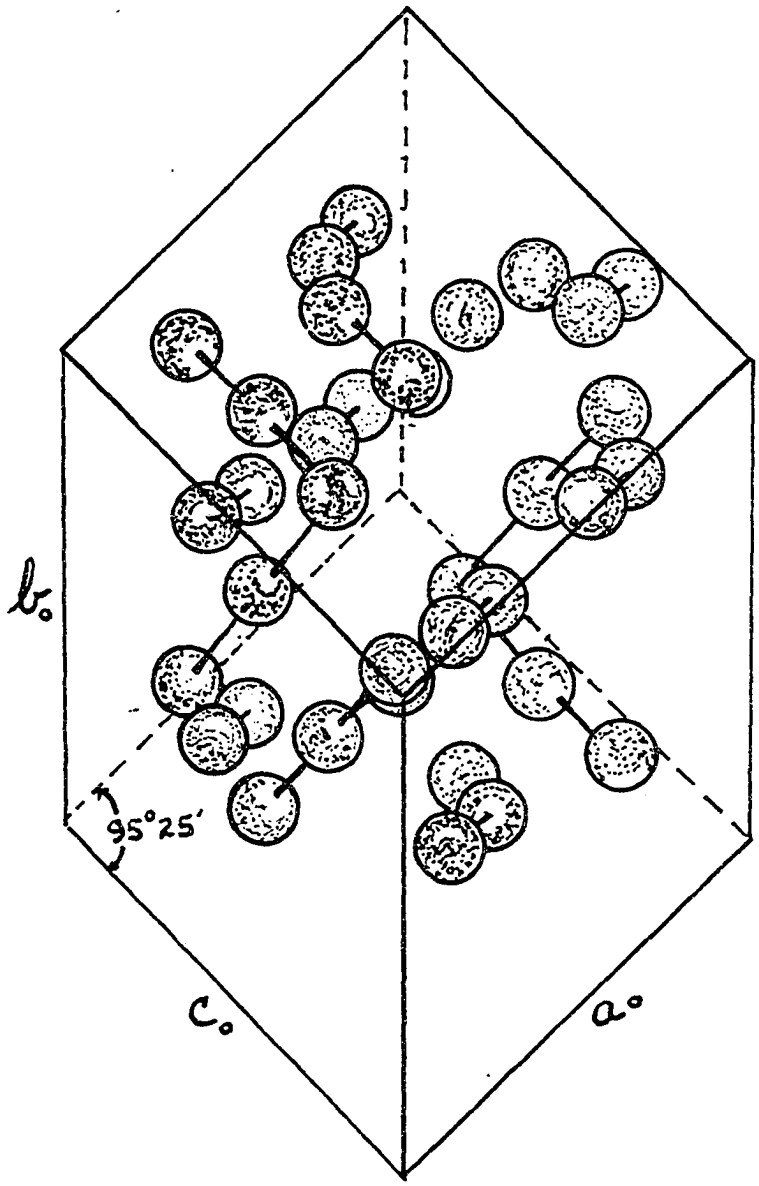
b₀
95°25'
c₀
a₀

Fig. 24 Projection of I_5^- net down the $a_o - c_o$ axis.

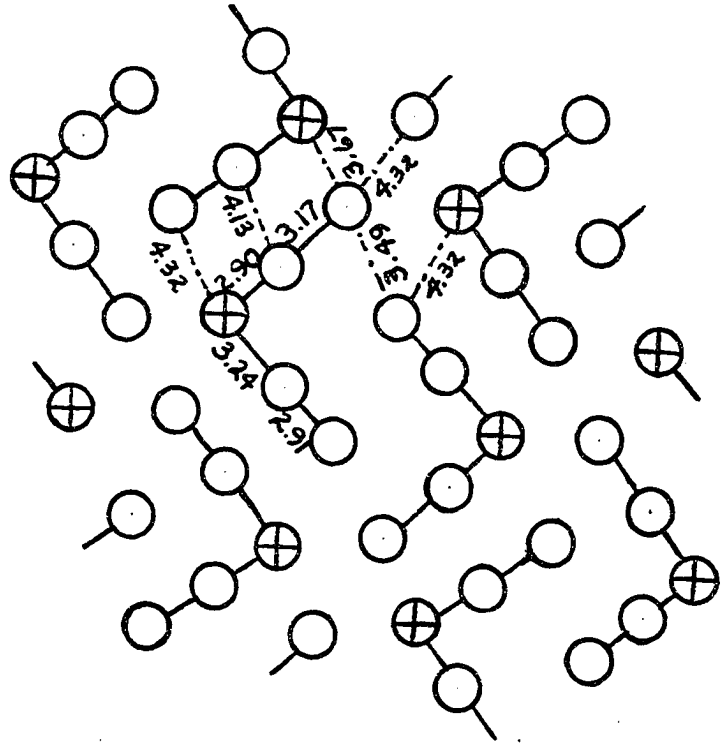
3.67
4.32
4.13
3.17
4.32
2.98
3.49
4.32
3.24
2.91

Fig. 25 Projection of one I_5^- net and I_2 molecules down $a_o - c_o$.


7
5
3
8
7
9
5
3
7
3
7
5
9
7
8
3
5
7

Fig. 26 Interaction of I_2 molecules with the I_5^-.

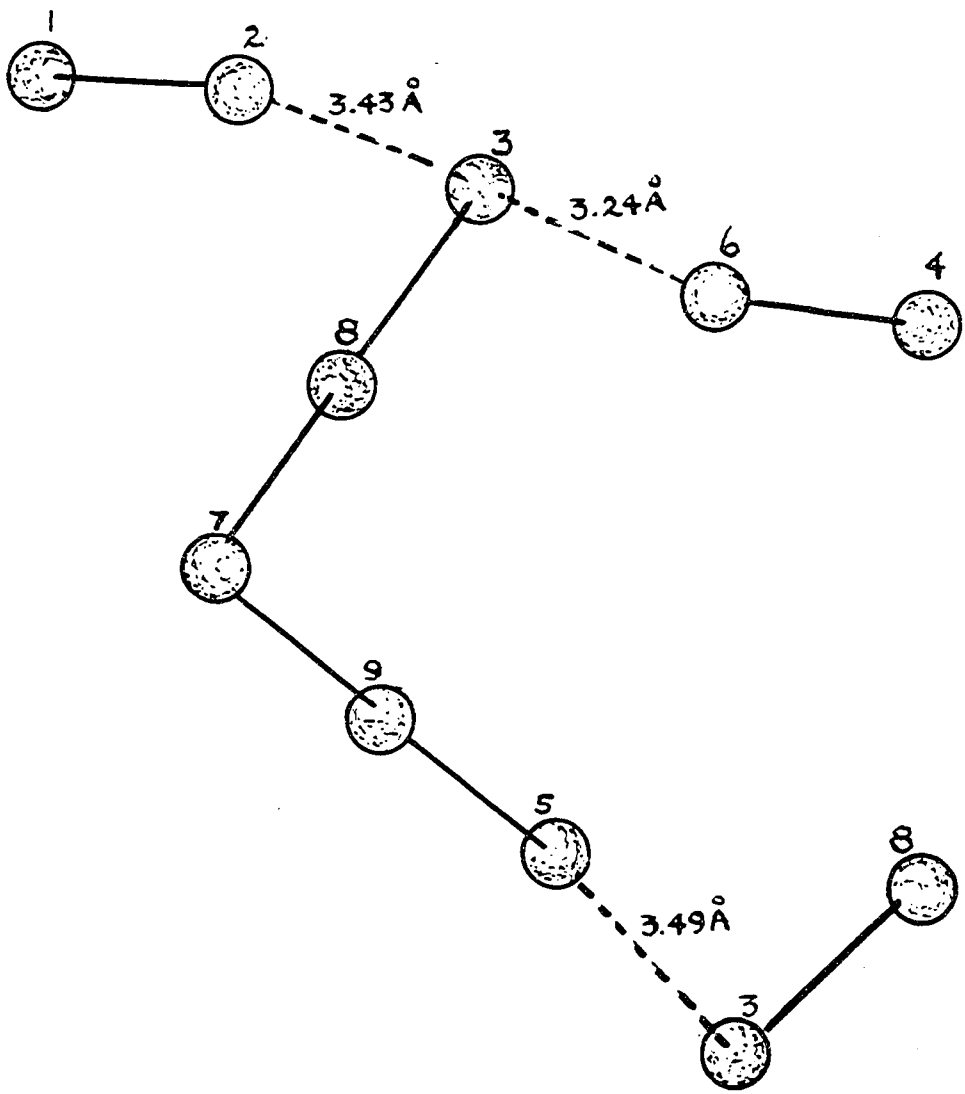
1
2
3.43 Å
3
3.24 Å
6
4
8
7
9
5
8
3.49 Å
3

is no apparent reason for this stronger interaction. In addition, the iodine-iodine bond distance in the molecule is only 2.67Å. Due to the polarizability of the I_2 molecule, a longer bond length would be expected. The I_2 molecule concerned is one in which difficulty has arisen in resolution of the atoms. Refinement of $hk\bar{l}$ data should be carried out before any conclusions concerning this short interaction can be made.

It is interesting that the I_5^- ions are not so well defined as in Hach and Rundle's structure. In Fig. 25, the distance between the terminal atoms 3 and 5 of the two pentaiodide ions is only 3.49Å so that one might consider the ion to be $I_{10}^=$. If the interactions of atom 3 with the I_2 molecules is considered, the structure may be described as I_7^- and I_2 or $I_{14}^=$ and two I_2.

The honeycomb arrangement of the iodine molecules is further shown in Fig. 27. Since the electron density of the cation constitutes only 9 percent of the total, no evidence for this ion would be expected in the Fourier projections. There are, however, large voids within the honeycomb arrangement which will readily accomodate the large positive ions. In addition, the occurrence of diffuse positive regions on all difference syntheses, which arise in the region of the voids, encourages this interpretation. If the cation is placed in a four-fold set with the nitrogen atom at $x = .367$, $y = .331$, and $z = .384$, the carbon atoms remain over 4.1Å from the iodine atoms, assuming the ideal angles of the tetrahedral configuration.

A glance at Fig. 25 will show that if the positive cation is placed in the center of the honeycombs, the charge is closer to atom 5 than to atom 3. Yet the negative charge apparently is not centered upon 5 but

Fig. 27 Arrangement of iodine molecules.

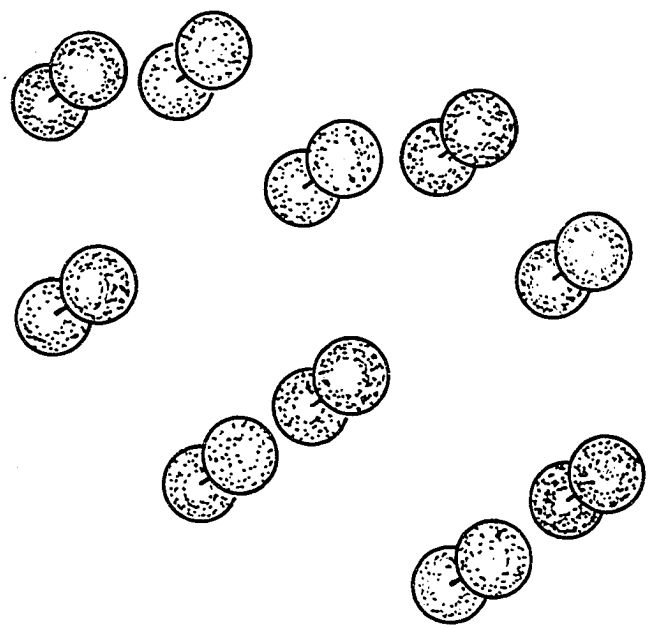

rather on 3. This is difficult to explain but the possibility may exist that the methyl groups are so positioned as to shield the effect of the cation on atom 5.

Errors

From the magnitudes of the R factors obtained, it is reasonable to believe that the interpretation given to this structure is correct. However, the magnitudes of the discrepancy factors have no bearing on the accuracy of the reported bond distances. The degree of accuracy in bond distances is essential to the problem if any significance is to be attached to the present interpretation.

Since the atoms in this structure are essentially all of equal weight and in general positions, the method of Booth for evaluating the standard error should be most satisfactory (36). Booth has shown that $nR_2 = \frac{\sum(|F_o| - |F_c|)^2}{\sum(F_o)^2}$, where n is equal to the number of dimensions in the summation, corresponds to the r.m.s. error. When the unobserved or zero reflections are included for the various two-dimensional data, $2R_2 = .044$ to .072, corresponding to an r.m.s. error of about .04 to .07Å.

Conclusions

Explanation of the nature of the bonding in the enneaiodide structure does not require the use of d-orbitals above the valence shell as used in ICl_2^- and ICl_4^-. The bond distances are considerably longer than would be expected for hybrid bonds involving the d-orbital. There can be little doubt that the distances in the pentaiodide ion of this structure are

appreciably greater than in I_2, and, in addition, that two different distances occur, just as was observed in I_3^- and I_5^- ions.

At this point it would be well to compare the pentaiodide ion of this structure with that reported by Hach and Rundle. In the latter the bonding between the end two iodine atoms of each arm of the V was observed to be stronger than the bonding between the apex iodine and the adjacent atoms, suggesting that two iodine molecules interacted with an iodide ion to form a weak covalent bond. This picture was extended to the linear I_3^- ion reported by Mooney. The unusual bond lengths obtained in the I_3^- and I_5^- ions were attributed to resonance between the usual covalent iodine-iodine bond and a longer interaction. The nature of the longer bond was ascribed to ion-induced dipole interaction arising from the polarizability of the iodine molecule.

These authors applied a simple molecular orbital argument to the I_3^- ion to show that resonance of the two forms $I^-\cdots I - I$ and $I - I\cdots I^-$ was reasonable without the use of d-orbitals. In the case of I_3^-, four electrons and three iodine p-orbitals were considered. By assuming that the Coulombic integrals and the exchange integrals for adjacent atoms were equal, the authors obtained a resonance energy of 0.828β.

By extending the resonance picture to the pentaiodide ion with the contributing forms as follows:

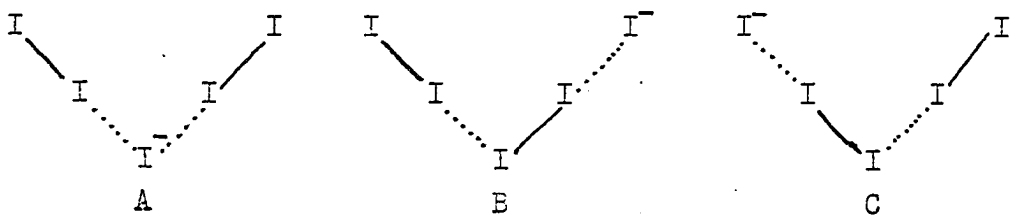

the authors were able to explain many of the questions which arise concerning the chemical behavior of the polyiodides. Each arm of the pentaiodide ion may be likened to the linear I_3^- ion. If a p-orbital of I^- is used in each arm of the I_5^-, the expected bond angle at the apex is 90° and the I_5^- ion should be planar. The V shaped ion was observed to have an apex angle of $94^\circ 0'$. The arms were linear within 4 degrees and the departure from planarity was only 0.12Å.

In the case of isolated I_3^- ions, contribution of each form in equal amounts will lead to a symmetric structure possessing the maximum degree of resonance energy. Since the I_3^- ion of Mooney is asymmetric, the explanation must lie in the fact that the cation lies nearer one end of the triiodide than the other, increasing the contribution of the resonance form with the negative charge nearer the cation.

As a result of the above, the authors were further led to suggest that as the cation in a polyiodide is made smaller, thus concentrating the positive charge, the resonating form with the negative charge closest to the positive charge will be dominant. If a sufficiently small cation could be obtained, a point would be reached where resonance stabilization would be very small. This explanation would account for the observation that small cations do not form polyiodides.

No significance can be attached to the variations in bond lengths observed between the two arms of the pentaiodide ion in the enneaiodide structure since these variations are less than the magnitude of error. It is interesting to note that the I_5^- ion in the enneaiodide structure does not have equal bond distances between the apex iodine and adjacent atoms as observed in the I_5^- ion of Hach and Rundle.

There is no reason to expect that both pentaiodide ions should be identical. The pentaiodide ions reported by Hach interact in pairs such as to accomodate the large positive ions, (Fig. 28). This packing arrangement allows the resonating negative charges to remain close to the positive charge and provides equal contribution of each resonating form.

The positive ion in the enneaiodide is not contained within voids formed by I_5^- ions but rather in the voids formed by I_2 molecules whose molecular axes are directed approximately normal to the planes of pentaiodide ions (Fig. 23).

An unequal field about the apex and arms of the V would certainly result in an unequal contribution of each resonating form. However, the author at this time is unable to explain the significance of the experimental bond lengths on the basis of the cation location. The contraction of the apex angle from 94.0° to 86.5° and the interlocking of the I_5^- ions within the net as shown in Fig. 24 is not surprising since this is what one might expect if the cation were made progressively larger or if more iodine molecules were added. The pentaiodide ion of Hach and Rundle must possess a larger apex angle to accomodate the large positive charge without distortion of the normal tetrahedral configuration of the cation.

A further study of this enneaiodide structure shows that the interaction of iodine molecules with I^- in the pentaiodide is weaker than in the I_5^- ion of Hach and Rundle. The difference in bond length is approximately 0.09Å greater in the enneaiodide. This may be explained by the fact that the location of the cation and the I_2 molecules is such as to increase the deviation of the I_5^- ions from planarity as evidenced by the experimental results. This increased departure from planarity may

Fig. 28 Structure of $N(CH_3)_4I_5$ (after Hach and Rundle).

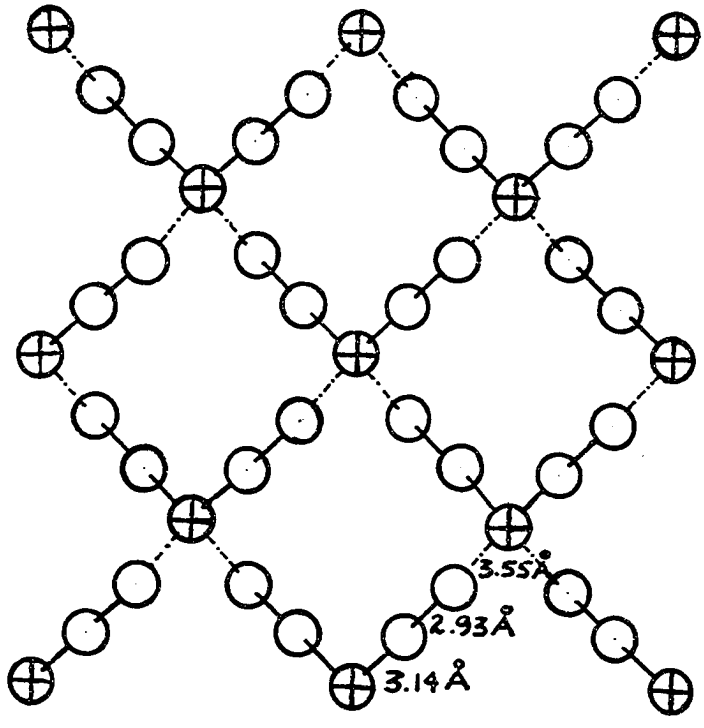
3.55Å
2.93Å
3.14Å

account for the weaker interaction of the iodine molecules with I^-.

In the structure of iodine each atom has a nearest neighbor at 2.67Å, which is the distance observed for the I_2 molecules in the enneaiodide structure. One would expect slightly longer bond distances because of the highly polarizable nature of I_2. Because of the error involved it is not unlikely that these lengths are indeed longer but there is no reason to expect bond lengths of the order of magnitude found in I_5^- ions.

The separation of the iodine atoms in adjacent I_5^- ions contained within essentially the same plane varies from 3.49Å to 4.3Å. These distances occur in the structure of iodine. However, the distance of 4.3Å is found as a layer separation in the iodine structure. In both structures the short van der Waals distance within the plane can be attributed to the strong interactions of the iodines due to the high polarizability in the direction of the bonds.

Suggestions for Further Study

The preceding discussion was not meant to constitute a complete substantiation of the views arrived at by the authors of the pentaiodide structure. Surely additional refinement by some other method such as least squares or by the more recent method of Cruickshank's (37) would be extremely valuable. Synthetic Fourier refinement making use of $(hk\bar{h})$ data might be most helpful. This author failed to note the advantages of refinement on this plane and is just now carrying out this refinement. One might expect better bond lengths from the $(hO\ell)$ data but this is questionable due to the large degree of overlap in this plane.

Spectrophotometric analysis of crystals of the polyiodide series may prove useful provided a suitable method can be found for preparing the crystals for analysis. Preparation of thin films of the compounds has been suggested but it is doubtful if they would be sufficiently transparent due to tendency of the higher polyiodides to deposit molecular I_2 on the surfaces.

It would be most interesting to carry out a structure determination for the heptaiodide ion. This ion does not crystallize with the tetramethylammonium ion but does form with the trimethylphenylammonium cation. It is quite possible that the heptaiodide ion consists of an I_2 molecule and a pentaiodide ion. If the cation should occupy one of the positions of I_2 in the enneaiodide structure, some similarity should exist between these two pentaiodide ions.

SUMMARY

Crystals of $N(CH_3)_4I_9$ are dark green monoclinic needles approximately rectangular in shape. The observed density is 3.47 gm/cc versus a calculated density of 3.51 gm/cc for a unit cell of $4N(CH_3)_4I_9$.

The lattice constants are $a_o = 11.60\text{Å}$, $b_o = 15.10\text{Å}$, and $c_o = 13.18\text{Å}$. The angle $\beta = 95°25'$. The space group is $P2_1/n$.

The iodine parameters expressed as fractions of the corresponding unit cell dimensions are as follows: $X_1 = .211$, $Y_1 = .058$, $Z_1 = .041$; $X_2 = .076$, $Y_2 = .084$, $Z_2 = .190$; $X_3 = .046$, $Y_3 = .800$, $Z_3 = .586$; $X_4 = .086$, $Y_4 = .416$, $Z_4 = .189$; $X_5 = .041$, $Y_5 = .318$, $Z_5 = .534$; $X_6 = .249$, $Y_6 = .400$, $Z_6 = .061$; $X_7 = .181$, $Y_7 = .084$, $Z_7 = .690$; $X_8 = .191$, $Y_8 = .729$, $Z_8 = .710$; $X_9 = .150$, $Y_9 = .455$, $Z_9 = .665$.

Fourier synthesis of four planes of data and refinement of the data indicate that the enneaiodide structure consists of iodine molecules packed with the cation and a pentaiodide ion. The structure might be best described as a honeycomb arrangement of I_2 molecules whose voids accomodate the positive ions which in turn separate planes of V shaped negative pentaiodide ions.

The bonding within the arms of the V shaped anions is quite different from that found in polyhalogens which contain two or more different halogens. Interpretation of the bonding does not require the use of d-orbitals above the valence shell. The bonding may be interpreted by means of a resonance picture as in the previously reported pentaiodide structure but the significance of the reported bond distances is still not clear.

The weaker interaction of the I_2 molecules with I^- in the planes of the

I_5^- net is attributed to the greater deviation from planarity of the anions as compared to the pentaiodide of Hach and Rundle.

The structure provides no evidence for believing that either the heptaiodide or enneaiodide constitutes the upper limits of the polyiodides.

LITERATURE CITED

1. Hanes, C. S., New Phytologist, 36, 189 (1937).
2. James, W. J., "X-ray Investigation of the Cyclohexaamylose-Iodine Complex", M. S. Thesis, Iowa State College Library, Ames, Iowa (1952).
3. James, W. J. and French, D., Proc. Iowa Acad Sci., 59, 197 (1952).
4. Wilson, A. J. C., Nature, 150, 151 (1942).
5. Booth, A. D., "Fourier Technique in X-ray Organic Structure Analysis", University Press, Cambridge, Cambridge, 1948, p. 104.
6. Karle, J. and Hauptmann, H., Acta Cryst., 5, 188 (1951).
7. Patterson, A. L., Z. Physik, 44, 596 (1927).
8. Wrinch, D., "Fourier Transforms and Structure Factors", The American Society for X-ray and Electron Diffraction, Vol. 2 (1946).
9. Ewald, P. P., Z. Krist., A90, 493 (1935).
10. Knott, C., Proc. Phys. Soc. Lond., 52, 229 (1940).
11. French, D., "An Investigation of the Configuration of Starch and Its Crystalline Degradation Products", Ph. D. Thesis, Iowa State College Library, Ames, Iowa (1942).
12. French, D., Levine, M. L. and Pazur, J. H., J. Am. Chem. Soc., 71, 356 (1949).
13. French, D. Unpublished research. Chemistry Department, Iowa State College, Ames, Iowa, 1952.
14. Geuther, A., Ann. Chemie., 240, 66 (1887).
15. Ludecke, O., Ann. Chemie., 240, 85 (1887).
16. Cremer, H. W. and Duncan, D. R., J. Chem. Soc., 2243 (1931).
17. Dawson, H. M. J. Chem. Soc. 93, 1308 (1908).

18. Dodson, R. W. and Fowler, R. D., J. Am. Chem. Soc., 61, 1215 (1939).

19. Buckles, R. E. and Popov, A. I., J. Am. Chem. Soc., 73, 4525 (1951).

20. Mooney, R. C. L., Z. Krist., 98, 324-377 (1938).

21. Pauling, L. C., "The Nature of the Chemical Bond", Second Ed., Cornell Univ. Press., Ithaca, N. Y., 1945, p. 111.

22. Mooney, R. C. L., Z. Krist., 90, 143 (1935).

23. Hach, R. J. and Rundle, R. E., J. Am Chem. Soc., 73, 4321 (1951).

24. Hach, R. J., "Structure and Chemistry of Polyiodide Compounds", Ph. D. Thesis, Iowa State College Library, Ames, Iowa (1952).

25. James, R. W., "The Optical Principles of the Diffraction of X-rays", Vol. II, G. Bell and Sons LTD, London, 1948, p. 376.

26. Harker, D. and Kasper, J. S., Acta Cryst., 1, 70 (1948).

27. Grison, E., Acta Cryst., 4, 489 (1951).

28. Hughes, E. W., Acta Cryst., 2, 34 (1949).

29. Zachariasen, W. H., Acta Cryst., 5, 68 (1952).

30. Sayre, D., Acta Cryst., 5, 60 (1952).

31. Cochran, W., Acta Cryst., 5, 65 (1952).

32. Cochran, W., Nature, 161, 765 (1948).

33. Finbak, C. and Norman, N., Acta Chem. Scand., 2, 813 (1948).

34. Booth, A. D., Proc. Roy. Soc. Lond., A197, 336 (1949).

35. Cochran, W., Acta Cryst., 4, 408 (1951).

36. Booth, A. D., "Fourier Technique in X-ray Organic Structure Analysis", University Press, Cambridge, 1948, p. 102.

37. Ahmed, F. R., and Cruickshank, D. W. J., Acta Cryst., 6, 385 (1953).

ACKNOWLEDGMENTS

The author wishes to express his grateful appreciation for the help and guidance of Drs. Dexter French and R. E. Rundle throughout this work.

The financial aid extended by Dr. Pepinsky of Pennsylvania State College and the use of his X-RAC machine were most appreciated. The author also wishes to thank Dr. Klaas Eriks, Dr. Elysiario Tavora, Dr. Qurashi, and Mr. Eiland for their helpful suggestions.

Thanks are due the Iowa Agricultural Experiment Station for financial assistance and last but not least the author gratefully acknowledges the work of Marion and Harold Smith in assembling this thesis.